

The relation between dense molecular clouds cores and very young stellar clusters

Hongjun Ma

@JCMT 2/27/2019

Outline

- Background
 - 1) Clusters forming
 - 2) Environment of clusters forming
 - 3) Method of cluster forming
 - 4) Star formation law
- Next steps
- Data

Background

Clusters forming

Gies DR. 1987

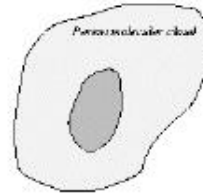
BINARY FREQUENCY

Type ^a	Cluster/Association	Field	Runaway
A. Visual Multiplicity			
VB	20	5	0
VMS	37	4	0
Total.....	42%	21%	0%
OPT	4	4	0
S	75	30	16
Total.....	58%	79%	100%

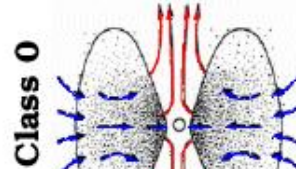
In the Milky Way Galaxy, for the global clustering of spectral O-type stars (Parker & Goodwin 2007), of which ~70% reside in young clusters or associations (Gies 1987) and ~50% of the remaining field population are directly identified as runaways (de Wit et al. 2005).

Low-Mass Stars

(after Lada 1987, Andre, Ward-Tompson & Barsony, 1993)
Prestellar Core

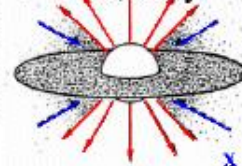


Submillimeter Protostar



Class 0

Infrared Protostar



Class I

T Tauri star



Class II

Evolved T Tauri



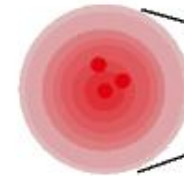
Class III

Massive Stars

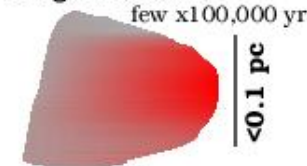
Prestellar Core(s?)



Hot Multi-Cores?



Ultra-Compact HII Region (UCHII)



OB Star (w/accretion remnants?)
<1 Myr

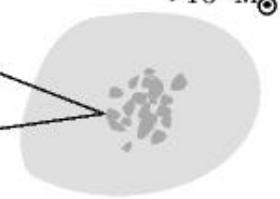


OB star

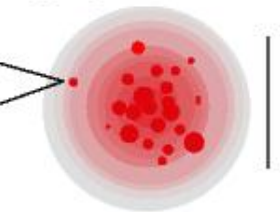


Massive Clusters

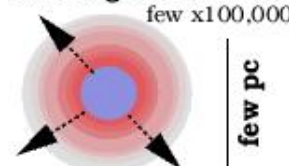
Massive Molecular Aggregates?
>10⁶ M_⊙



Massive Submillimeter Aggregates?



Massive Ultra-Dense HII Regions (UDHII)
few x100,000 yr



Young Super Starcluster

1-3 Myr



Super Starclusters
-> Globular Clusters?

3 Myr - 13 Gyr

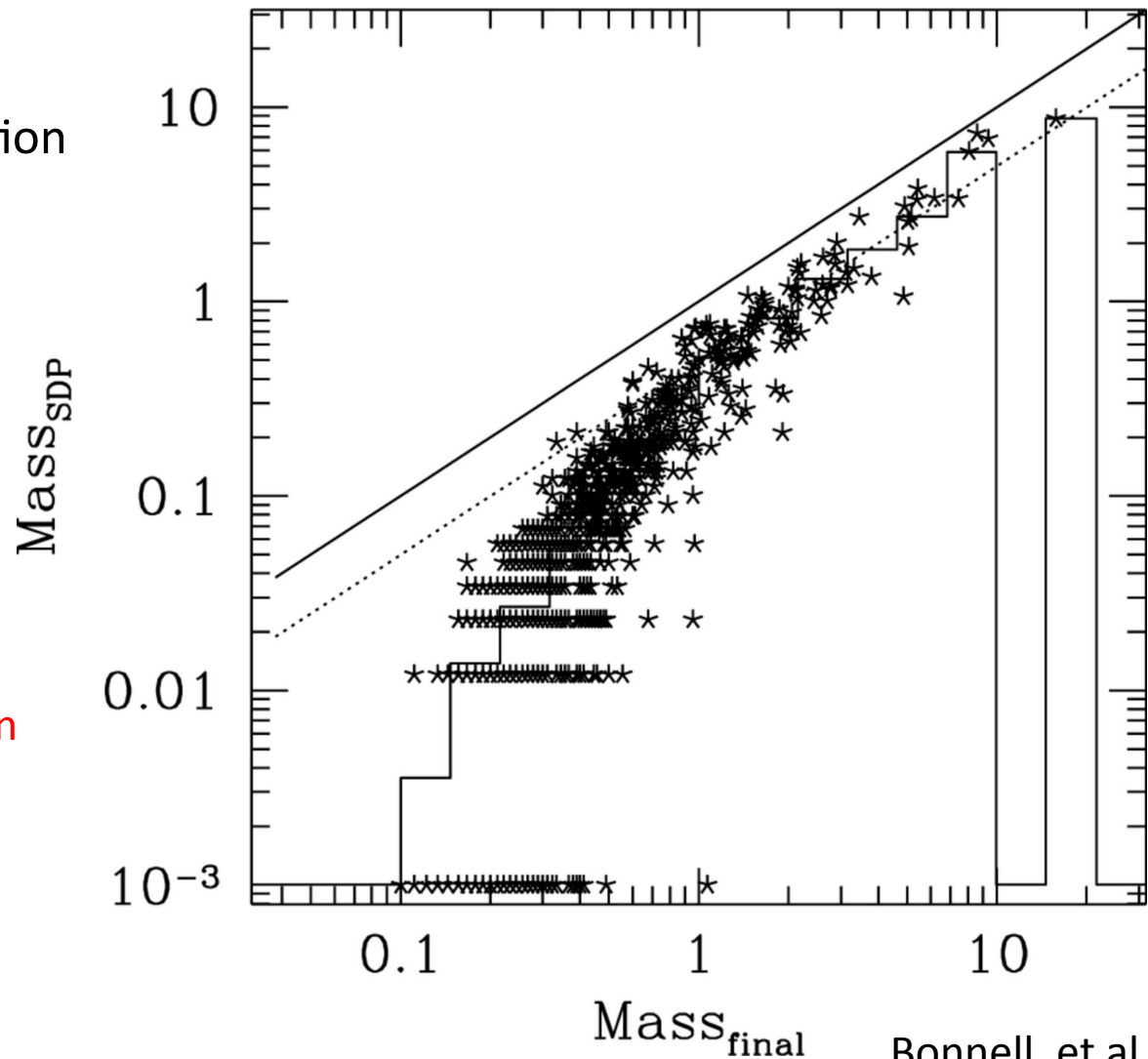


Method of cluster forming : fragmentation or accretion

Simulations of accretion in clusters containing 1000 stars result in mass spectra broadly consistent with these analytic estimates.

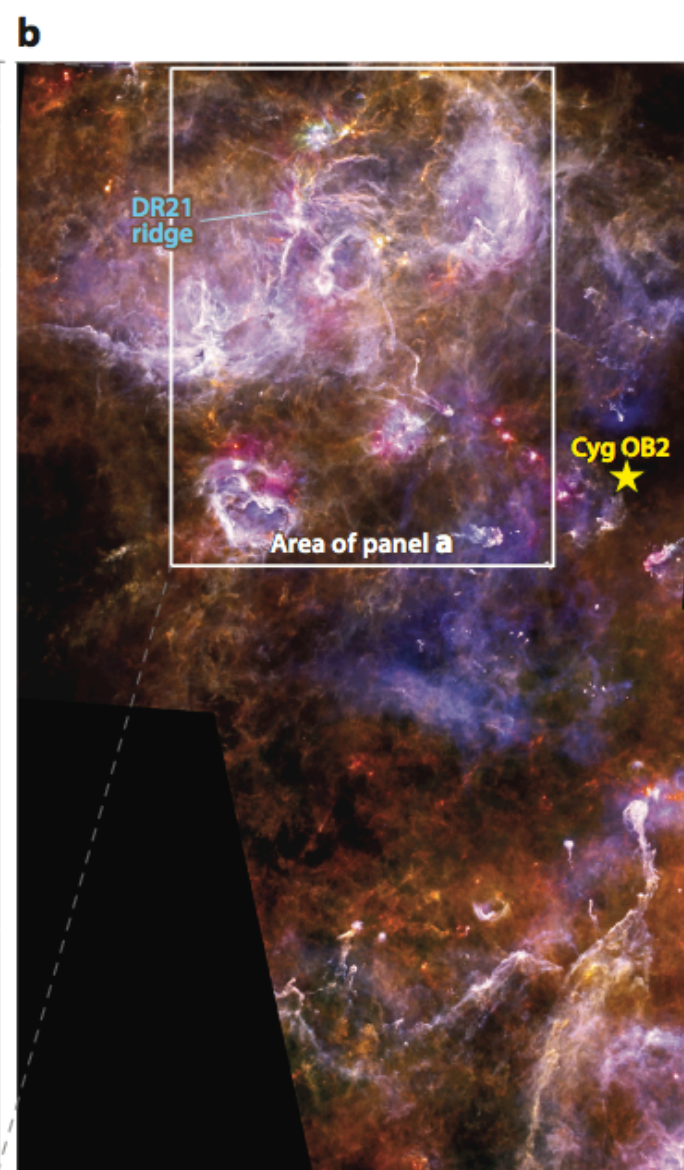
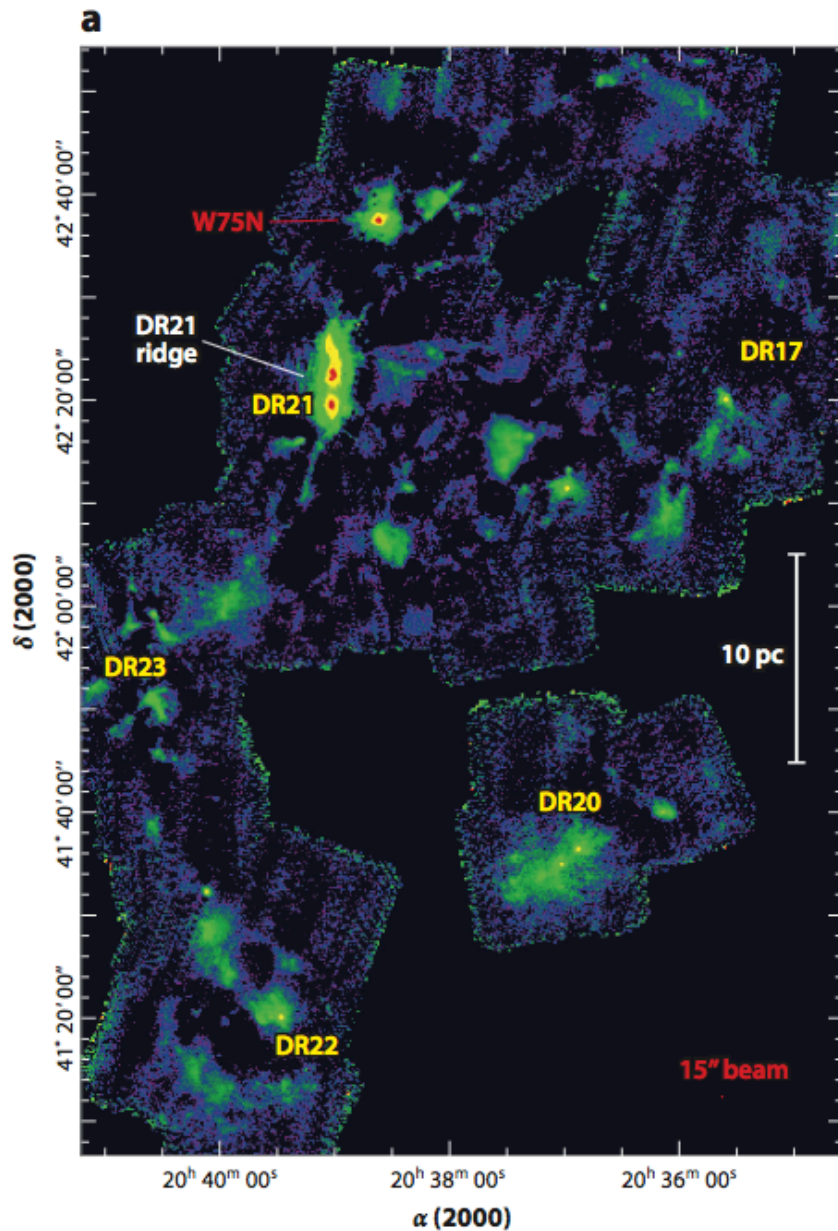
The high-mass stars are confirmed to accumulate the majority of their mass in a stellar-dominated potential.

Lastly, competitive accretion in clusters naturally results in mass segregation as the accretion rates are higher near the cluster centre during the gas-dominated phase.



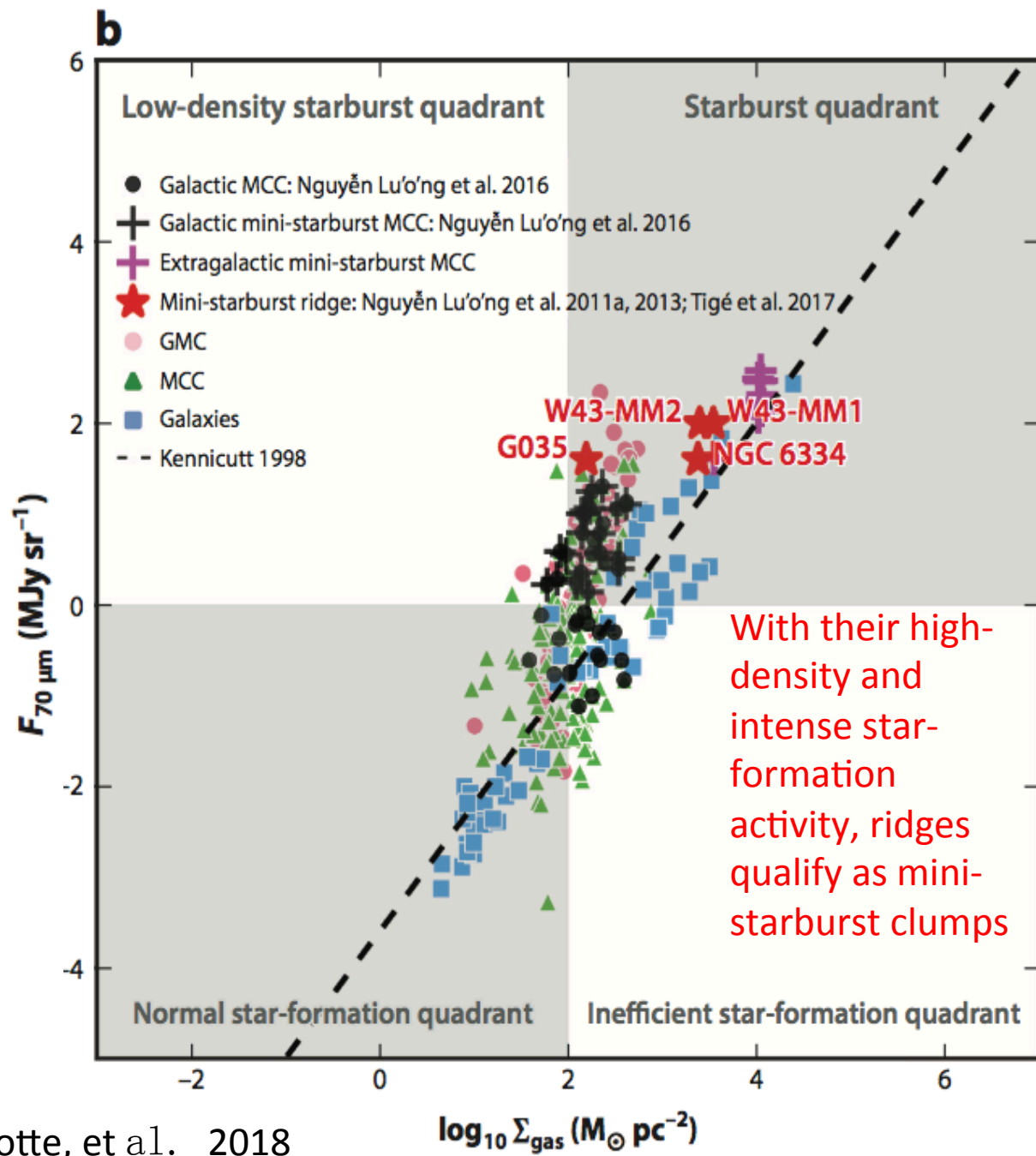
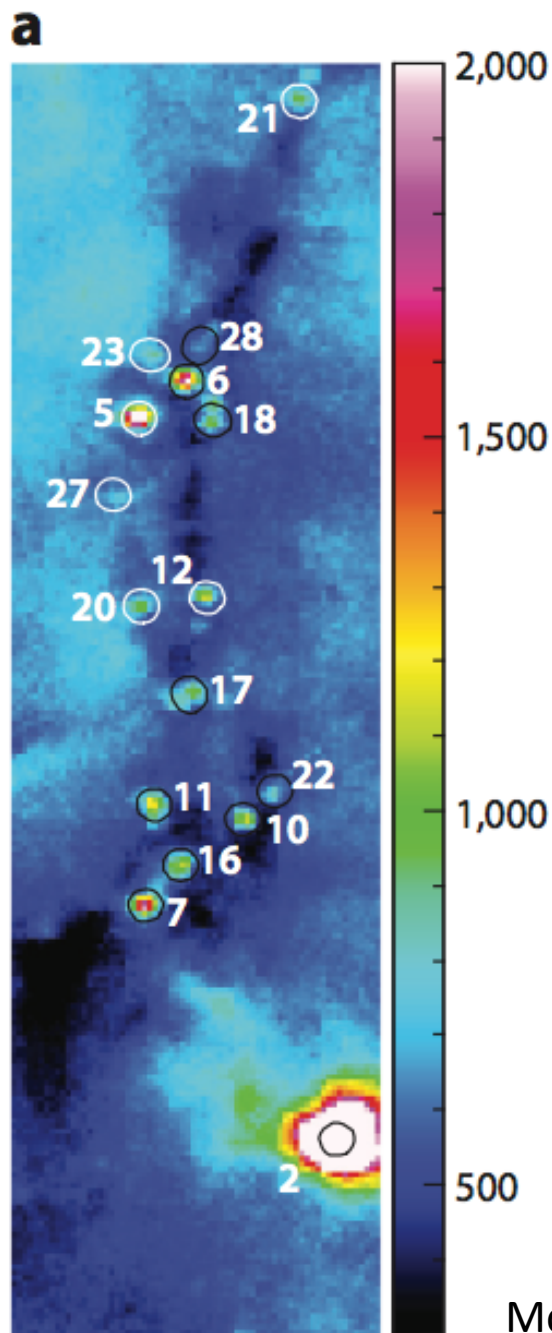
The mass accreted during the stellar-dominated phase, $Mass_{SDP}$, plotted against total stellar mass

Environments of cluster forming



Motte, et al.
2018

The extreme characteristics of ridges and hubs, in terms of density and kinematics, could lead to atypical star-formation activity.



High-mass stars form in molecular complexes hosting massive clouds and often OB clusters. Parsec-scale massive clumps/clouds called **ridges and hubs** are the preferred, if not the only, sites for high-mass star formation. Their infall velocity and density structure suggest ridges/hubs undergo a global but controlled collapse.

high-mass star formation develops simultaneously and in tight link with the formation of massive clouds and massive clusters

Motte, et al. 2018

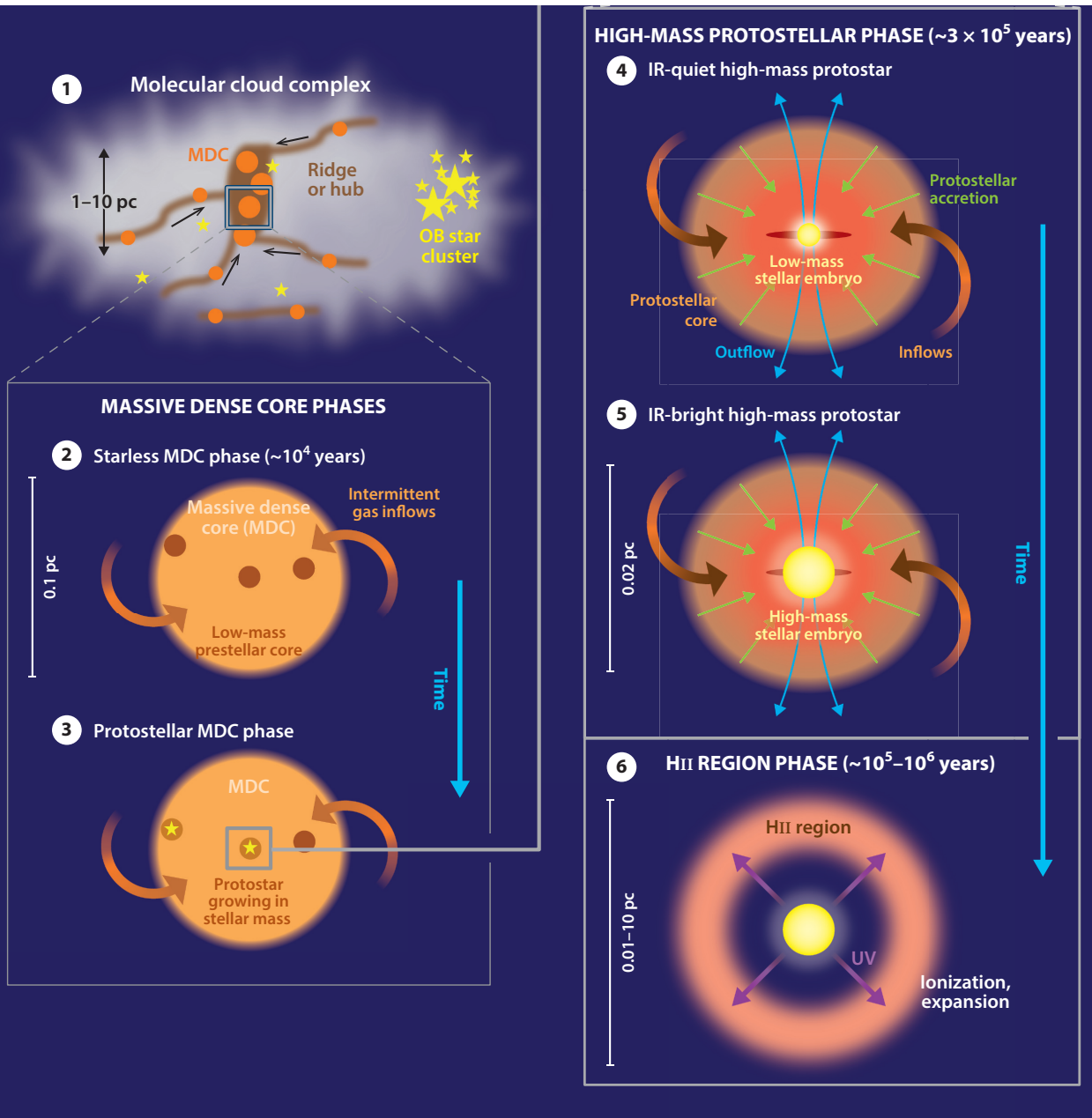
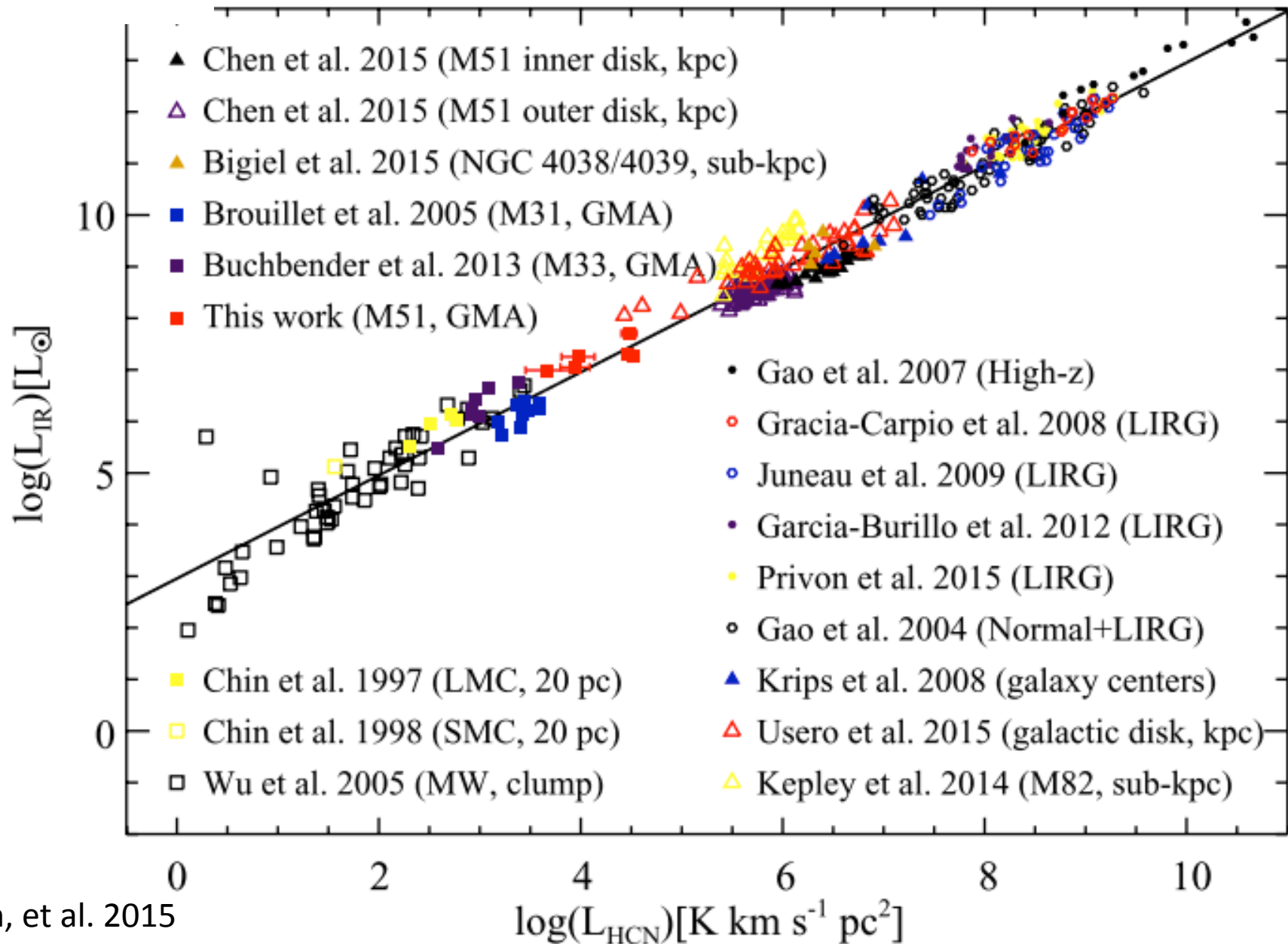


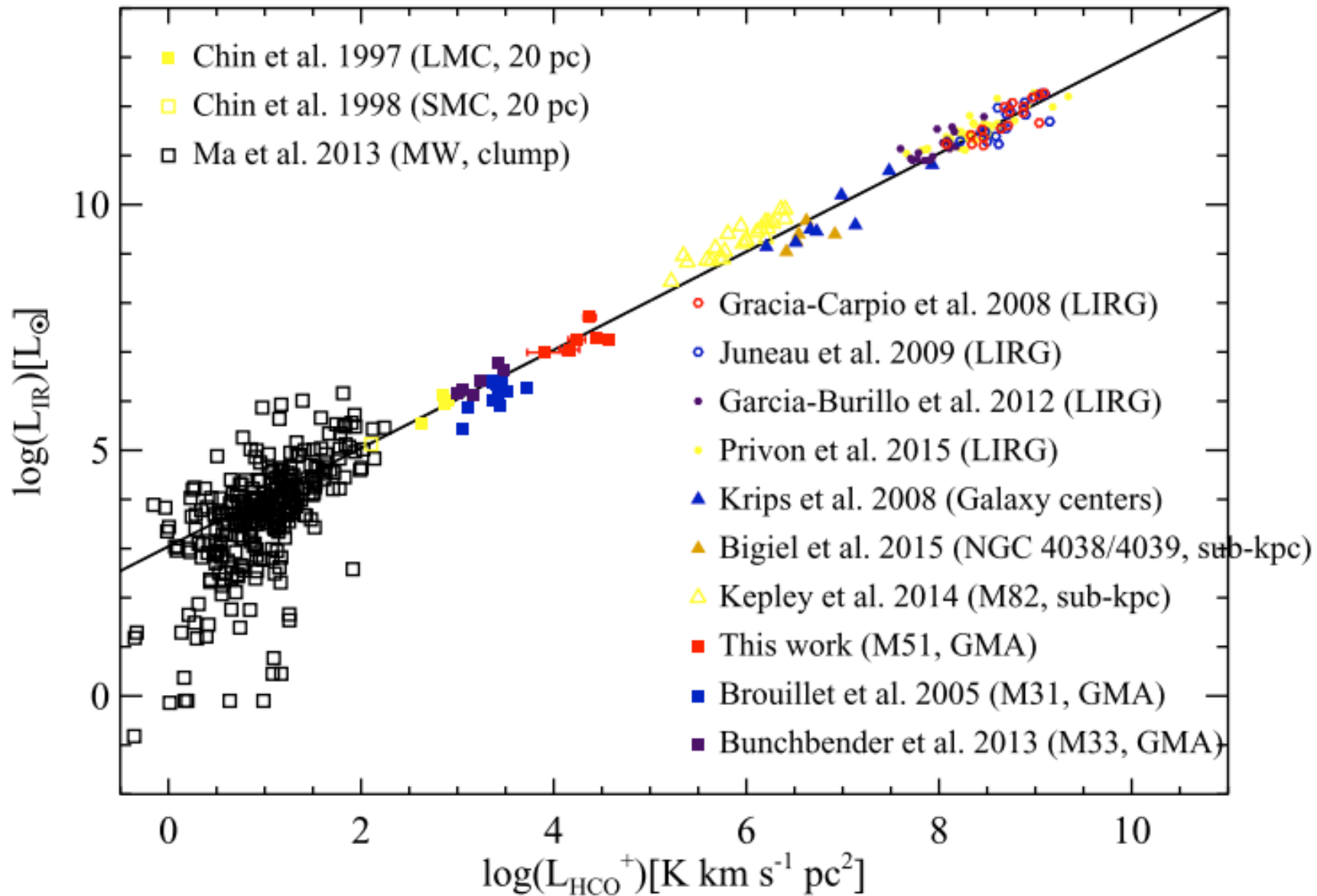
Figure 8

$$\Sigma_{SFR} \propto (\Sigma_{gas})^n$$

star formation law (SFL--KSL)



star formation law



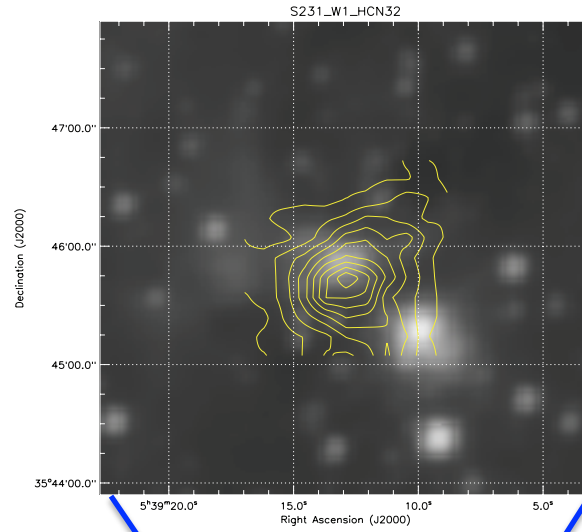
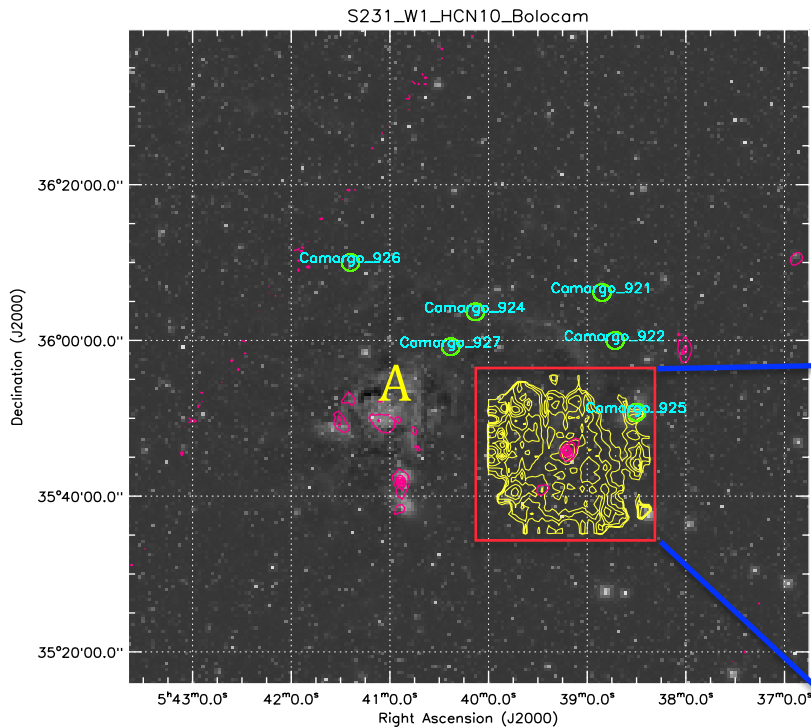
Our sample

- Wu et al. 2010 (82 molecular cloudy cores – massive star forming regions)
- Kharchenko et al. (2005) & Piskunov et al. (2008) —more than 3000 Galactic open clusters
- Camargo et al. (2011, 2015)—1089 embedded stellar clusters

About 40 molecular cloudy cores with young stellar clusters around

Sample: GMCs with young stellar clusters around

S231 observing



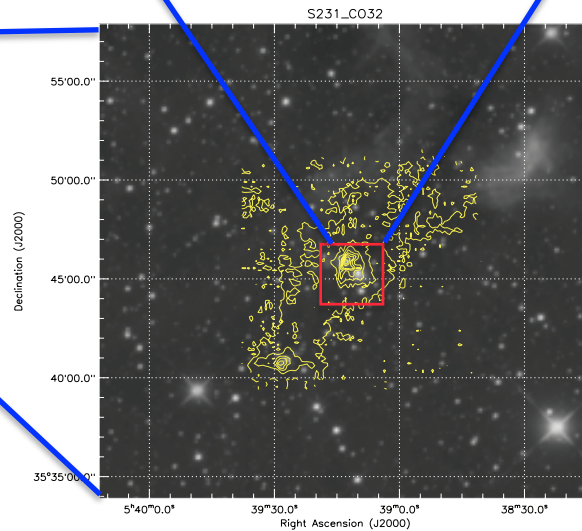
CSO HCN(3-2)

S231 pink is Bolocam
1.1 mm;

Cyan is Camargo et
al. (2011, 2015)
clusters

JCMT CO(3-2)
contour map.

Background is WISE
3.4 micron band
image.



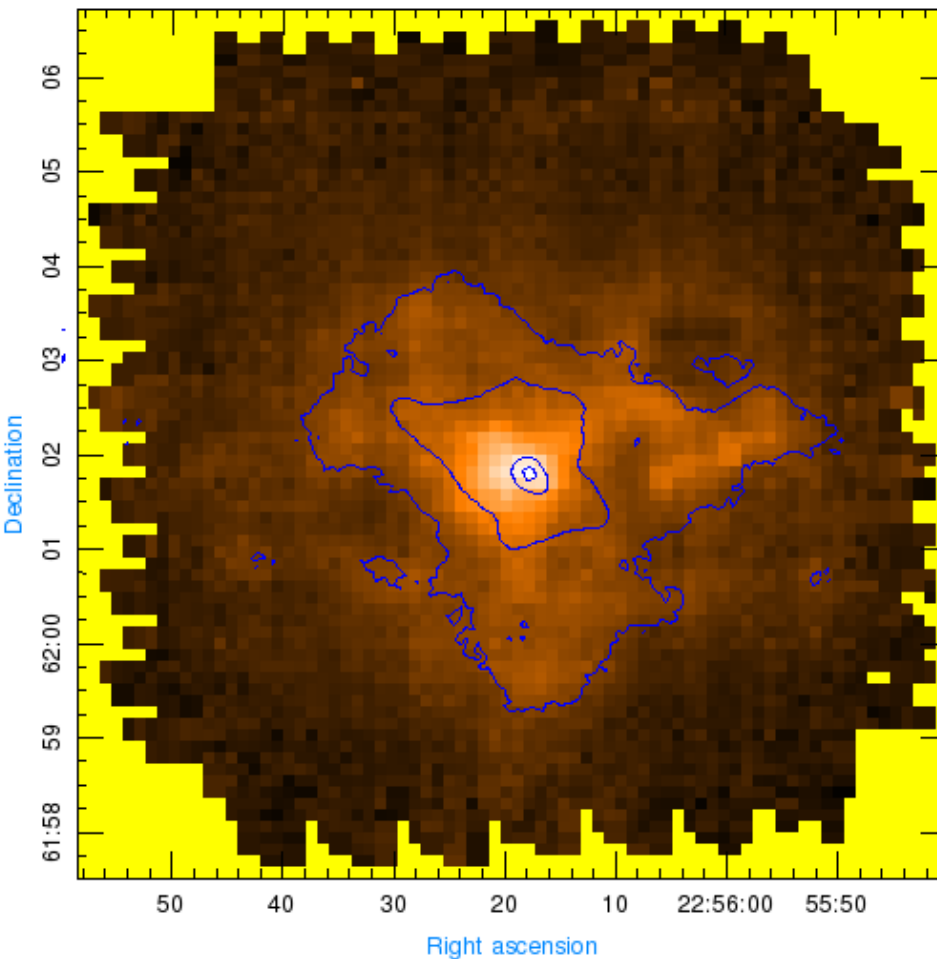
S231 Yellow contours is HCN(1-0) observing
with DLH telescope ;

The sample with JCMT CO and Scuba-2 archive data available

# Name	RA	Dec	equ	Scanline	line2	project_1	850mic	project_2
W44	18:53:18.5	01:14:56.2	J2000	HCN(4-3)	0	0	scuba-2	0
S106	20:27:25.7	37:22:51.8	J2000	HCN(4-3)	0	0	scuba-2	0
W3(OH)	02:27:04.7	61:52:25.5	J2000	13CO(3-2)	C180(3-2)	M07BU16	scuba-2	S14BC01
NGC7538	23:13:44.85	61:26:50.67	J2000	13CO(3-2)	C180(3-2)	M07BU16,	scuba-2	M16BP006
S158	23:13:44.9	61:26:50.6	J2000	13CO(3-2)	C180(3-2)	M07BU16	scuba-2	M15BI059
S158A	23:13:45.4	61:28:11.7	J2000	13CO(3-2)	C180(3-2)	M08AU19	scuba-2	M15BI059
NGC7538-IRS9	23:14:01.7	61:27:19.9	J2000	13CO(3-2)	C180(3-2)	M07BU16	scuba-2	M15BI059
S157	23:16:04.4	60:01:40.6	J2000	13CO(3-2)	C180(3-2)	M10BU08	scuba-2	M13AU03
W75N	20:38:36.9	42:37:37.5	J2000	13CO(3-2)	C180(3-2)	M08AU19	scuba-2	M11BEC30
W75(OH)	20:39:01.01	42:22:49.9	J2000	13CO(3-2)	C180(3-2)	M08AU19	scuba-2	M11BEC30
S255	06:12:53.7	17:59:22.1	J2000	13CO(3-2)	C180(3-2)	M08BU18	scuba-2	M11BD02
CEP_A	22:56:18.1	62:01:46.2	J2000	13CO(3-2)	C180(3-2)	M08BU18	scuba-2	M13AU03
W51	19:23:04.16	14:36:25.90	J2000	13CO(3-2)	C180(3-2)	M08AU06	scuba-2	M16AP046
W51W	19:23:11.0	14:26:38.1	J2000	13CO(3-2)	C180(3-2)	M08AU06	scuba-2	M16AP046
W51M	19:23:43.9	14:30:29.4	J2000	13CO(3-2)	C180(3-2)	M08AU06	scuba-2	M16AP046
w43North	18:47:36	-01:57:00	J2000	13CO(3-2)	C180(3-2)	M10AC06	scuba-2	S13AU02
W43_Main3	18:47:47.2	-01:54:35.1	J2000	13CO(3-2)	C180(3-2)	M10AC06	scuba-2	MJLSJ02
w43South	18:46:00	-02:42:00	J2000	13CO(3-2)	C180(3-2)	M10AC06	scuba-2	MJLSJ02
S231	05:39:12.9	35:45:54	J2000	13CO(3-2)	C180(3-2)	M11BN07	scuba-2	MJLSY02
W3(2)	02:25:40.6	62:05:51.1	J2000	13CO(3-2)	C180(3-2)	M07BH45B	scuba-2	M13BC07
RCW142	17:50:14.7	-28:54:31.6	J2000	13CO(3-2)	C180(3-2)	M15A118	scuba-2	M12AJ01
W28A2(1)	18:00:30.4	-24:03:58.5	J2000	13CO(3-2)	C180(3-2)	M09AU13	scuba-2	M12AJ01
W33cont	18:14:13.7	-17:55:25.2	J2000	13CO(3-2)	C180(3-2)	M10BD02	scuba-2	MJLSJ02

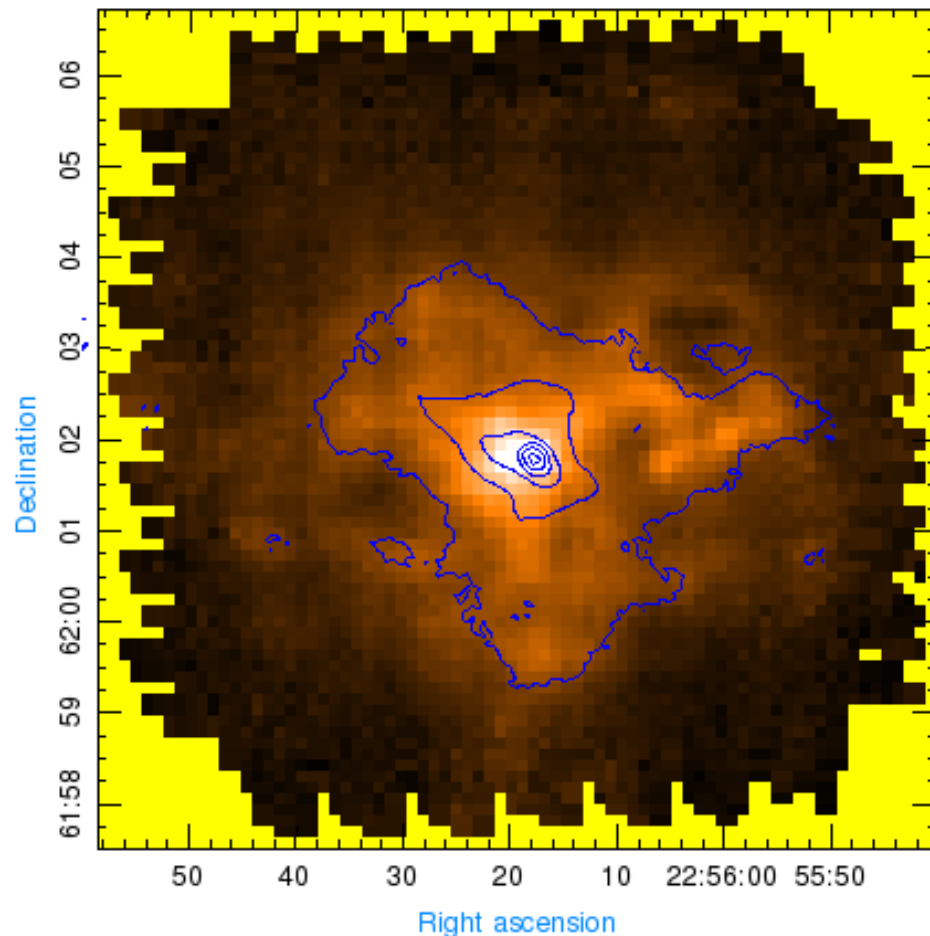
Cep A

Cep A_13co_850



Range of velocity of CO (-20 _ 0)

Cep A_13co(-20_0)_850



Back ground grey map: ^{13}CO (3-2) observed with HARP;
contour map are 850 micron emission observed with SCUBA -2

850 micron emission contour level:
49.5037, 26.5168, 3.52986, 0.5

850 micron emission contour level: 50.7693,
39.3769, 27.9845, 16.5921, 5.19972, 0.5

Next steps

◆ Stellar clusters

- 1) to identify the new clusters with WISE data
- 2) check the age of all the clusters including the clusters published in literature

◆ Molecular cloudy core

- 1) getting the Mass of GMC cores with ^{13}CO (3-2) data
- 2) getting physical parameters of GMC cores with other dense gas tracers data

◆ Comparing the Initial Mass function (MF) of clusters with the MF of GMC cores

- 1) getting the mass function of GMC cores with simulation method
- 2) try to get more high resolved data to get the Mass function of GMC cores
- 3) try to get the Initial MF of clusters with optical and IR data.

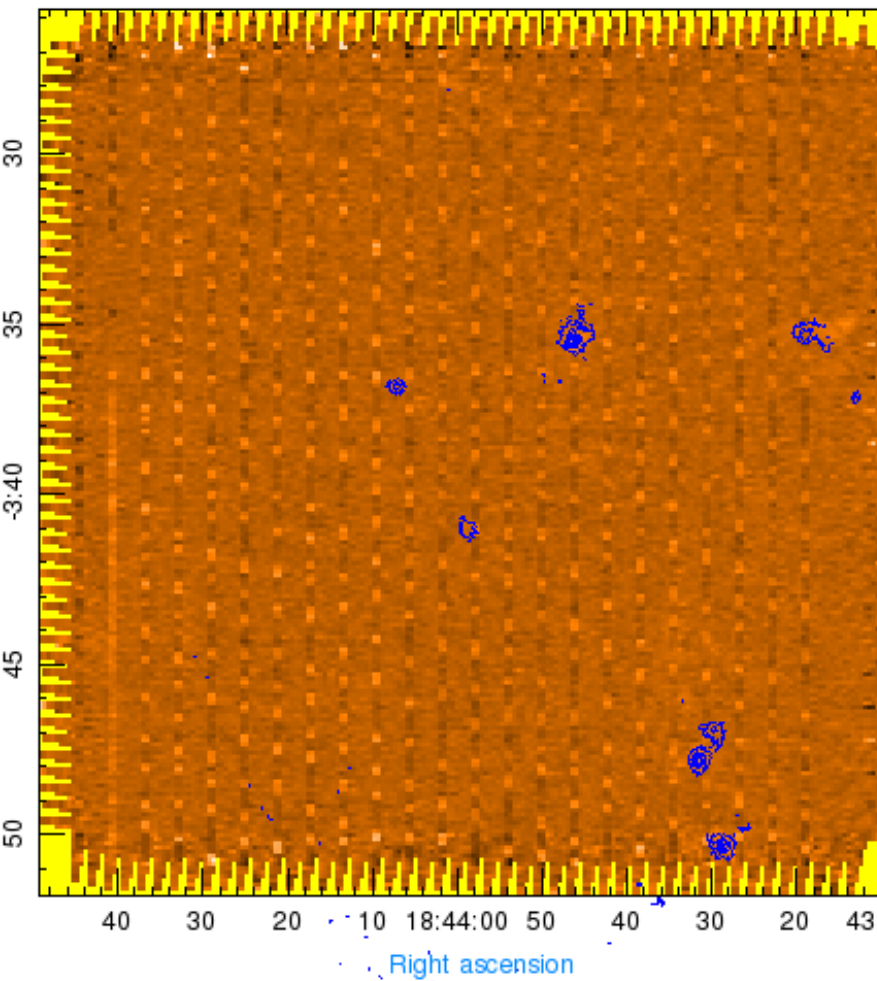
◆ Checking SFL with star clusters

- 1) getting the luminosity of CO (3-2) of the molecular cloudy cores
- 2) identify the distance of clusters with gaia data to remove the front and back clusters
- 3) getting the mass of clusters to check the SFL

G28.86+0.07

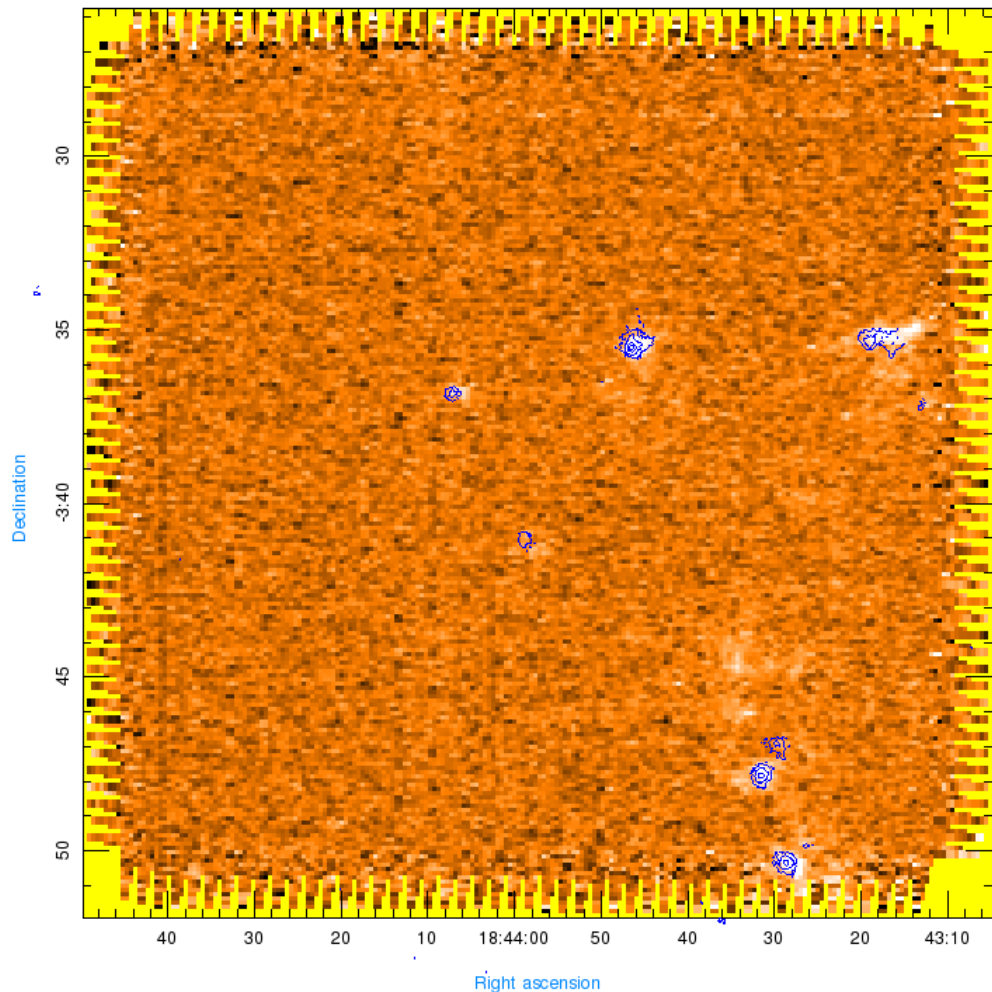
Range of velocity (96 _ 110)

G28.86+0.07_13co_850



The contour level: 1.74429, 4.27113, 6.79797, 9.32482, 12

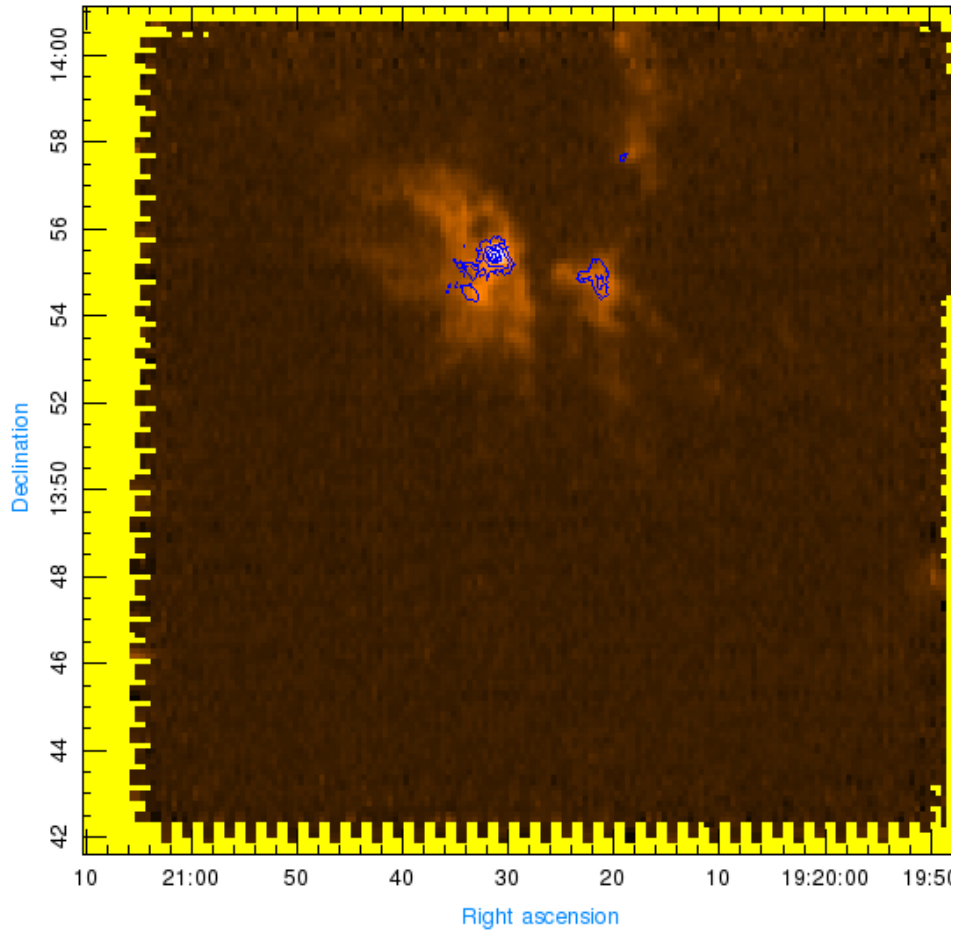
G28.86+0.07_13co(96_110)_850



The contour level: 2, 4.27113, 9.32482, 12

G48.61+0.02

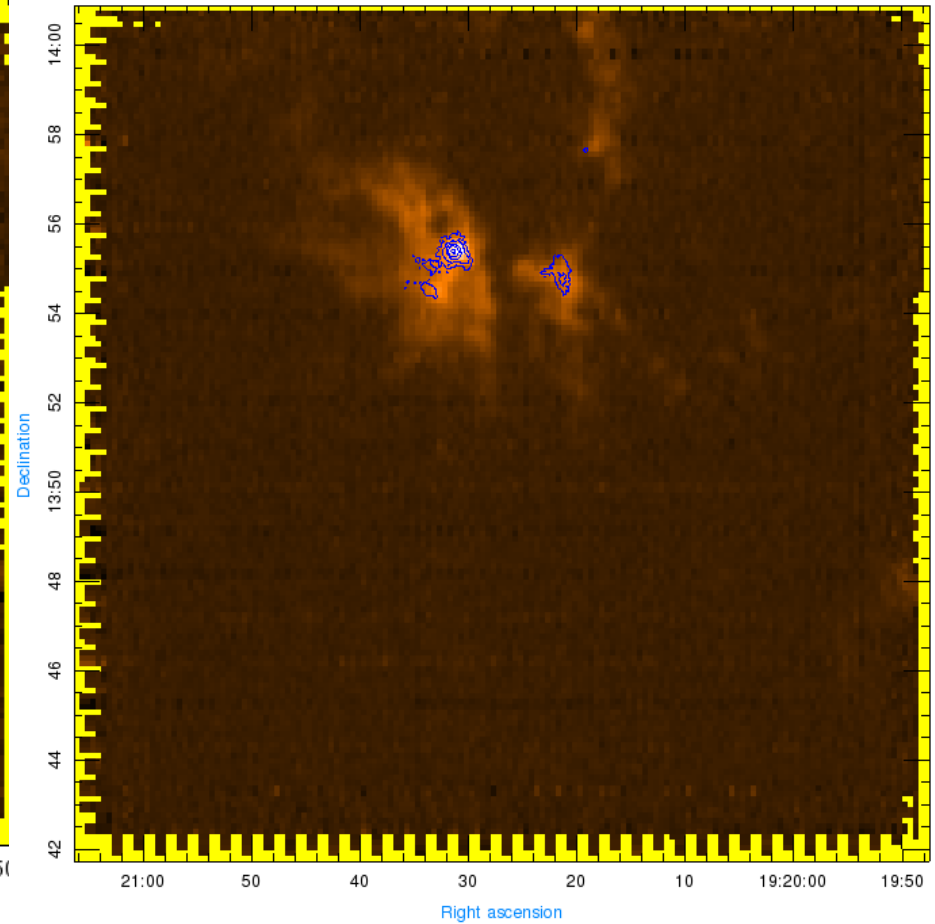
G48.61+0.02_13co_850



The contour level: 14, 10, 7, 4, 2.5

Range of velocity (6 _ 26)

G48.61+0.02(6_26)_13co_850



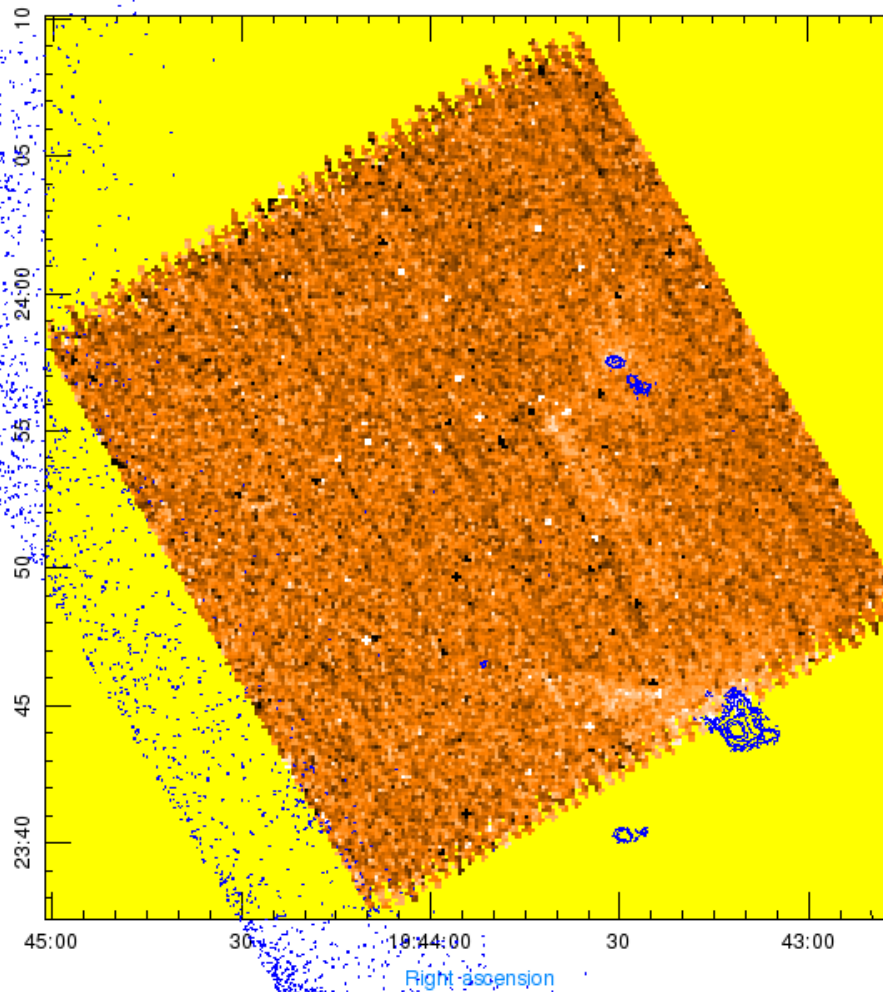
The contour level: 14, 10, 7, 4, 2.7132

G59.78+0.06

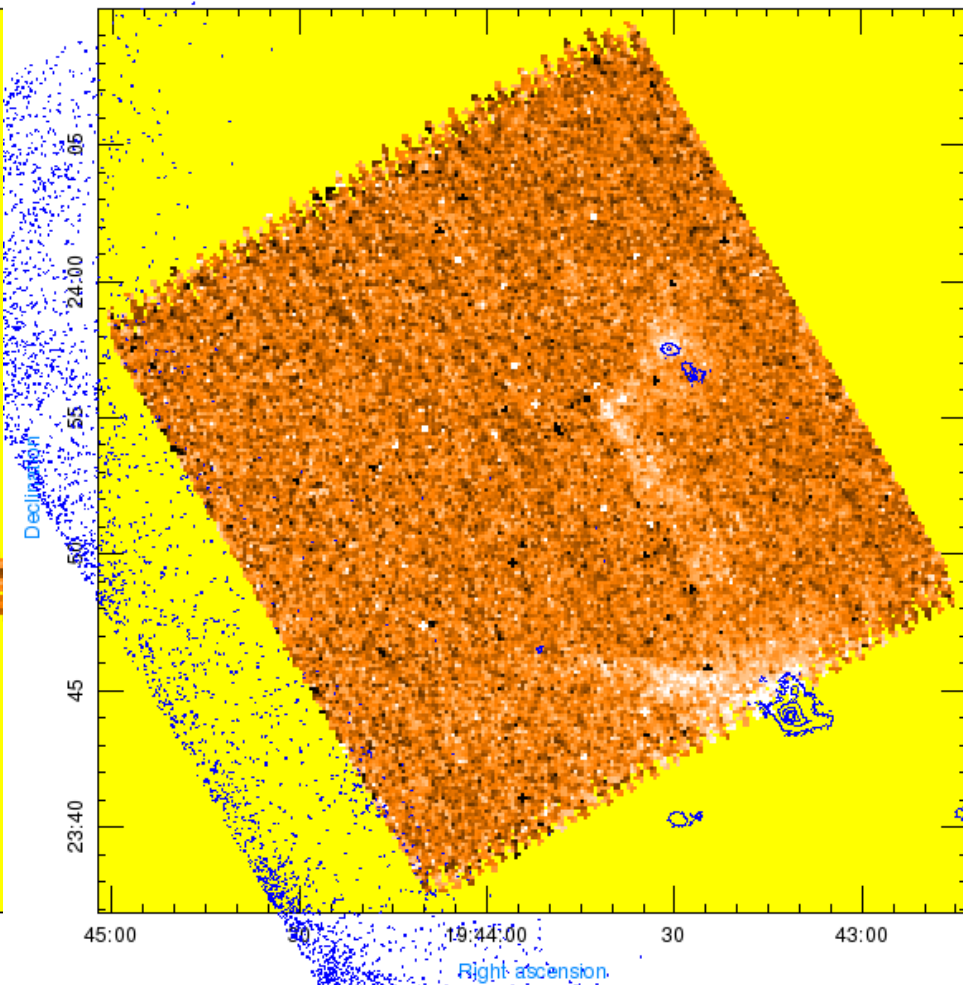
G59.78+0.06_13co_850

Range of velocity (18_28)

G59.78+0.06_13co(18_28)_850



The contour level: 7, 5, 3, 1.5, 1



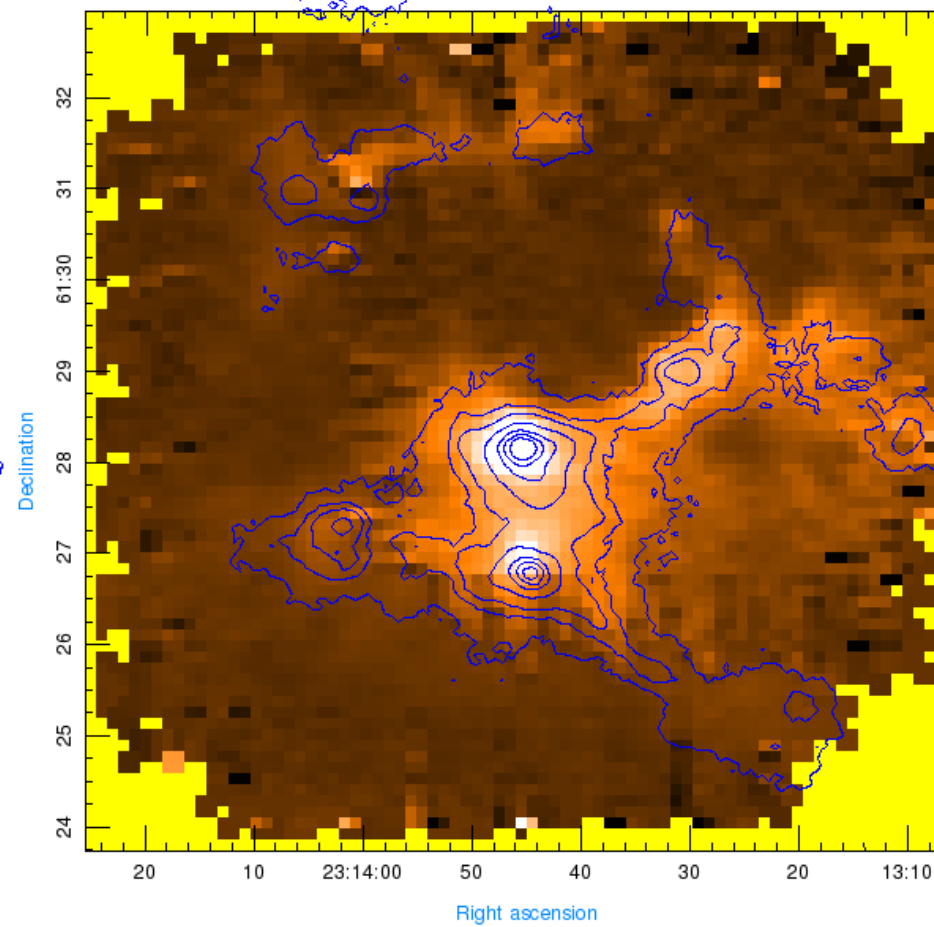
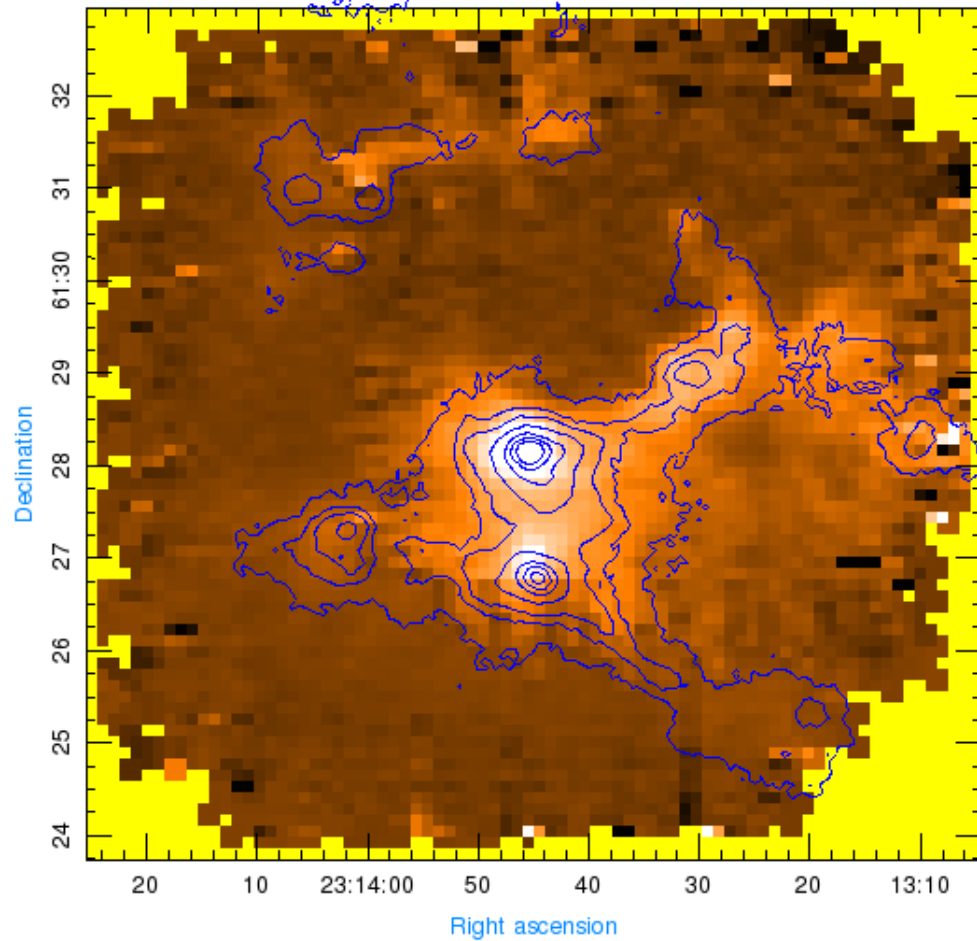
The contour level: 12.4829, 9.42406, 6.38524, 3.34642, 1

NGC7538

Range of velocity (-70_ -40)

NGC7538_13co_850

NGC7538_13co(-70_-40)_850



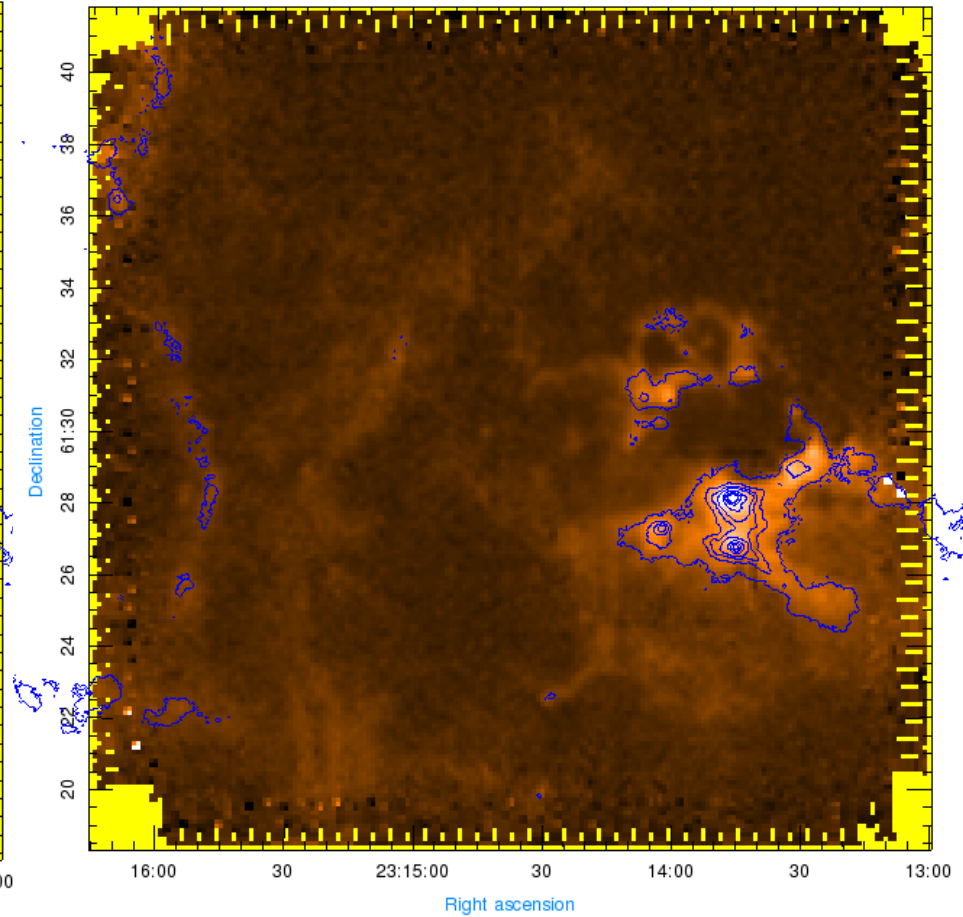
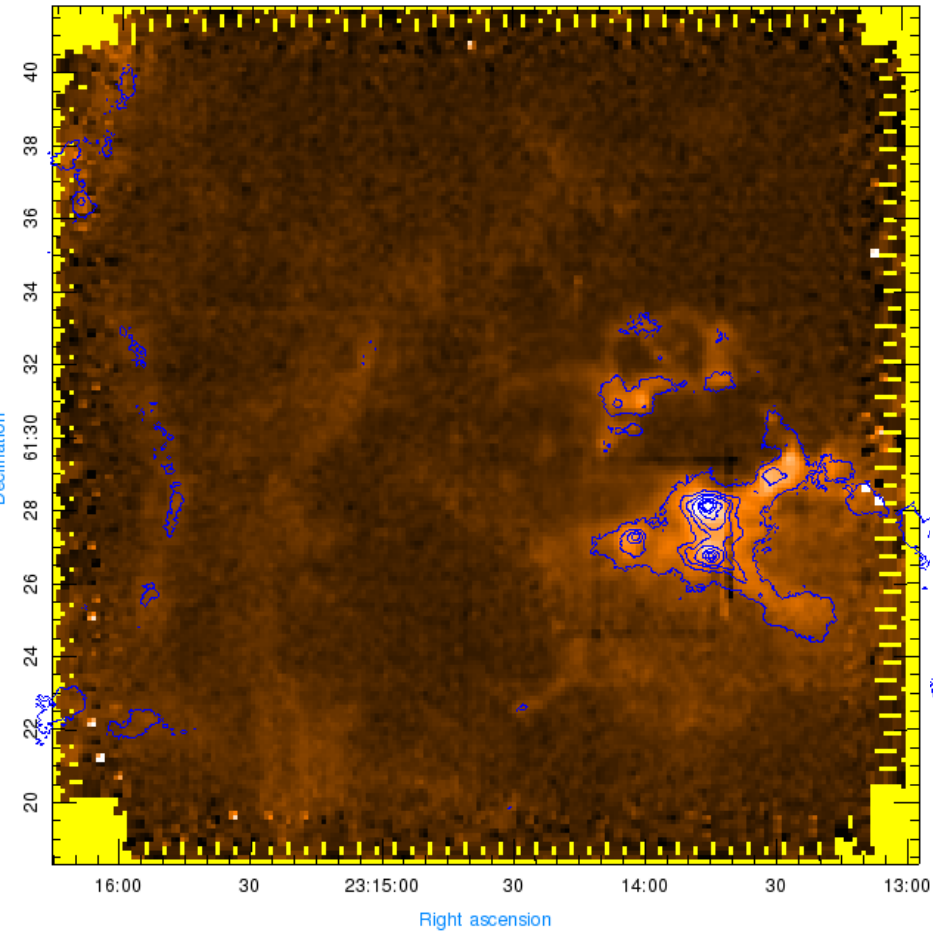
The contour level: 39.729, 29.8928, 20.0588, 10.2204, 5, 3, 1

NGC7538-IRS9

Range of velocity (-70 _ -42)

NGC7538-IRS9_13co_850

NGC7538_IRS9_13co(-70_-42)_850

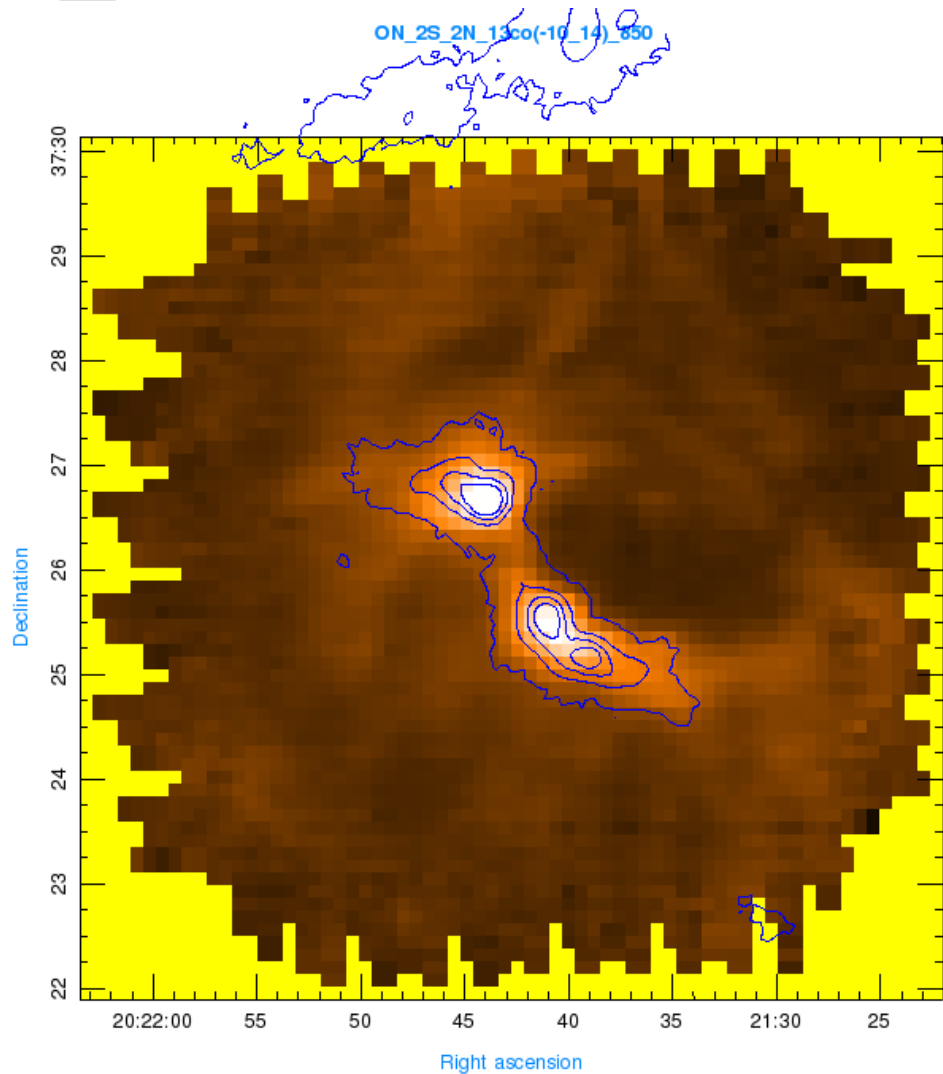
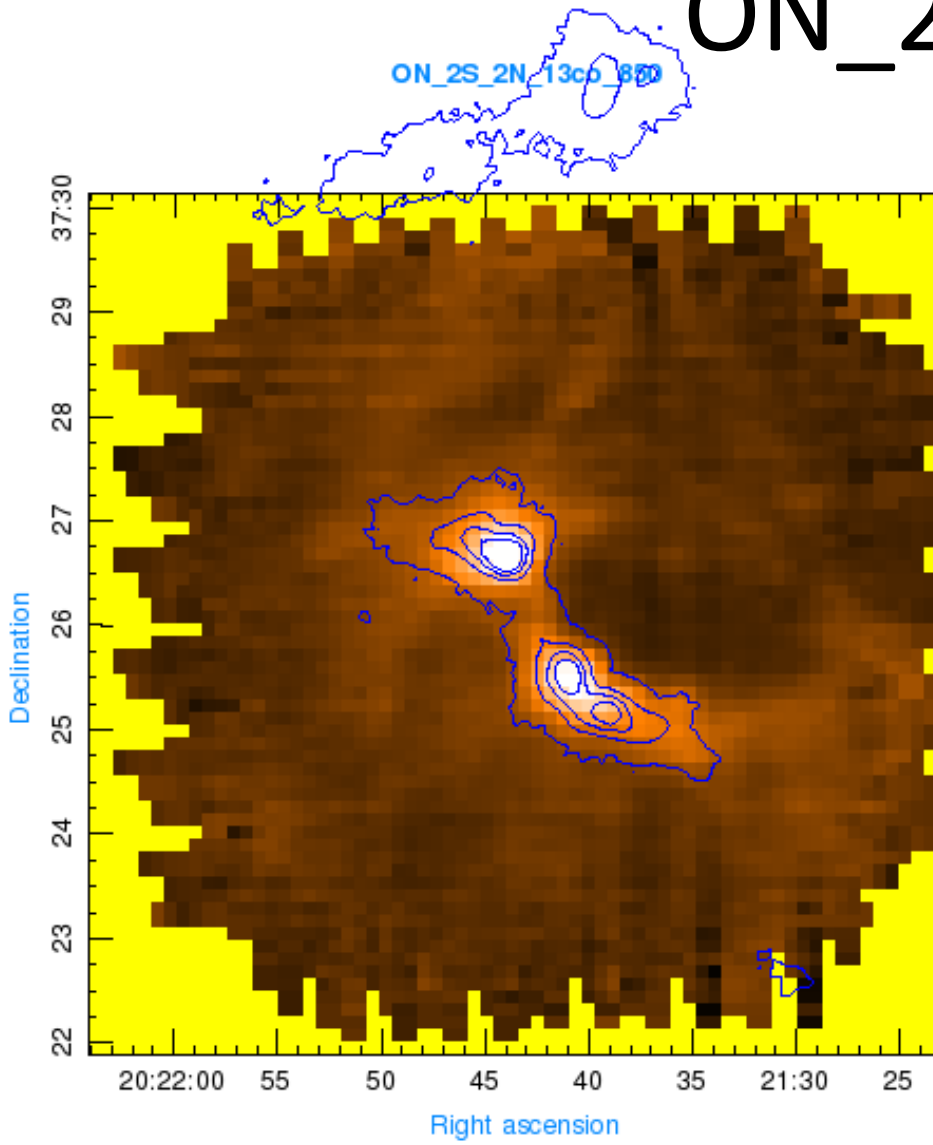


The contour level: 39.729, 29.8928, 20.0588, 10.2204, 5, 3, 1

The contour level: 39.729, 29.8928, 20.0588, 10.2204, 7, 4, 1

ON_2S_2N

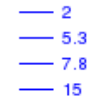
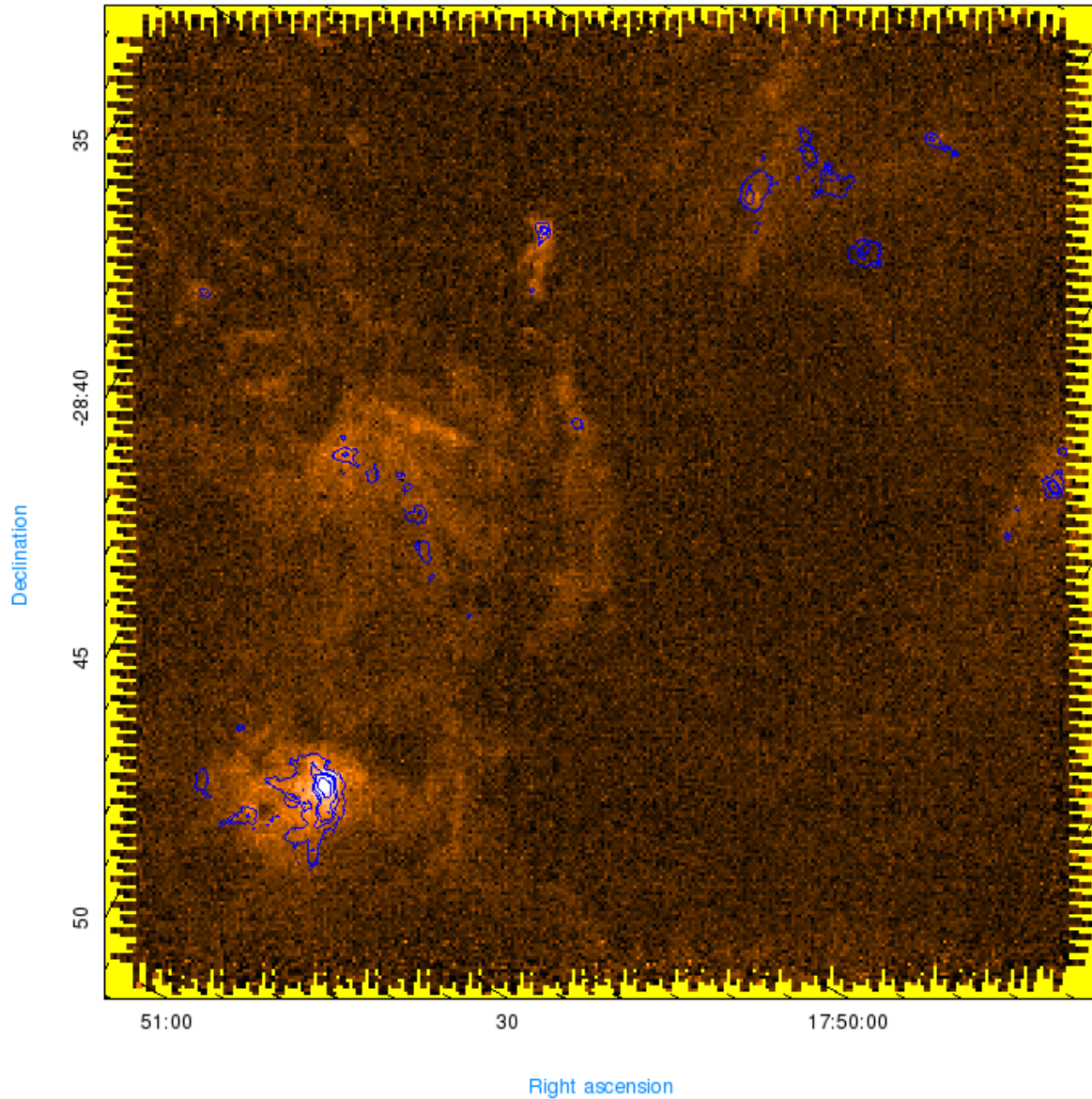
Range of velocity (-10 _ 14)



The contour level: 14.479, 10.233, 5.98703, 1.74102

RCW 142

RCW142_13co(8_30)_850

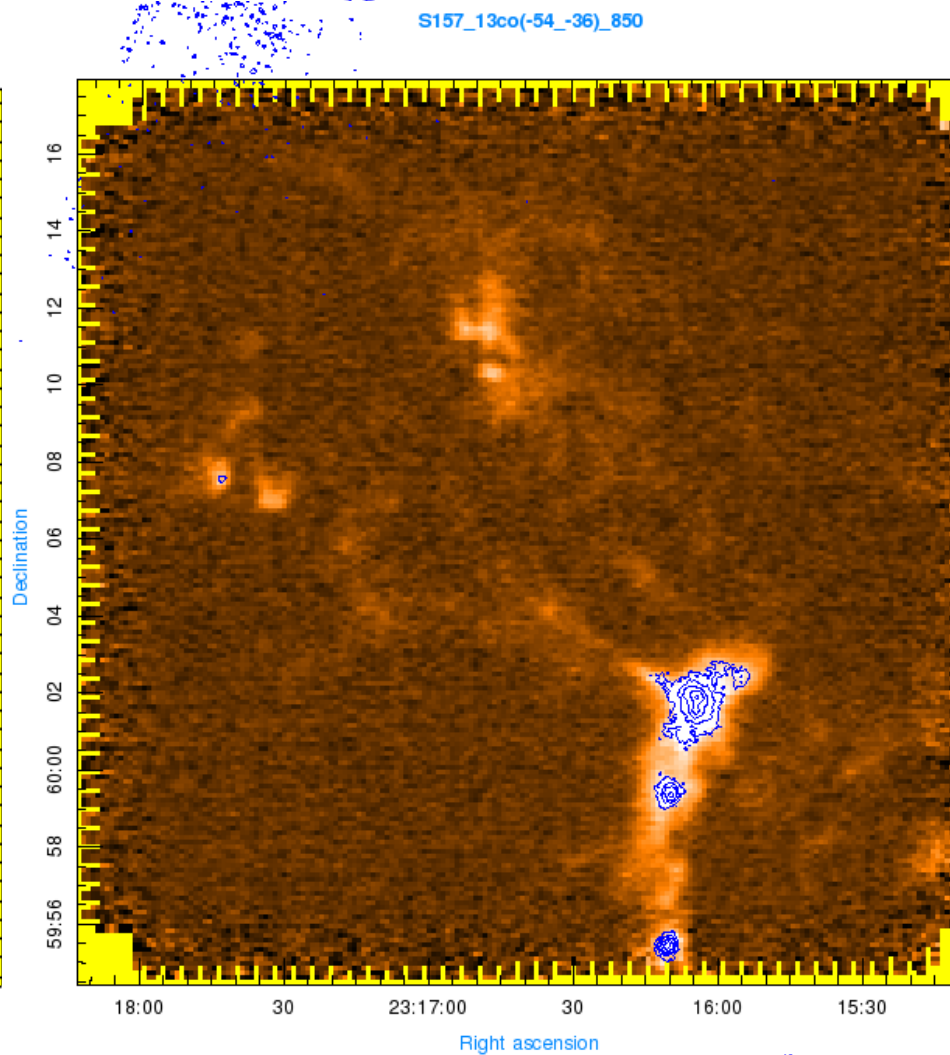
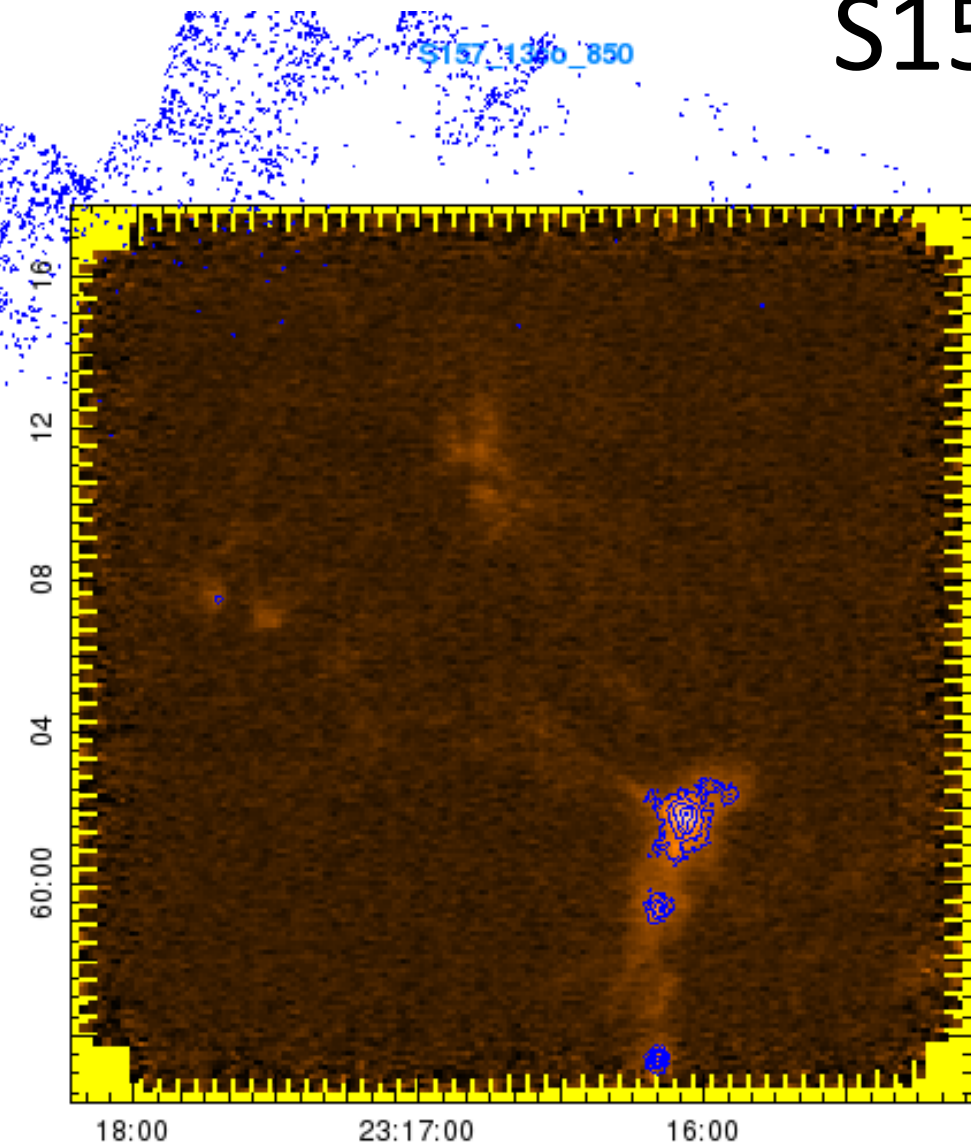


Range of velocity (8 _ 30)

The contour level: 15, 7.8, 5.3, 2

S157

Range of velocity (-54 _ 36)



Right ascension

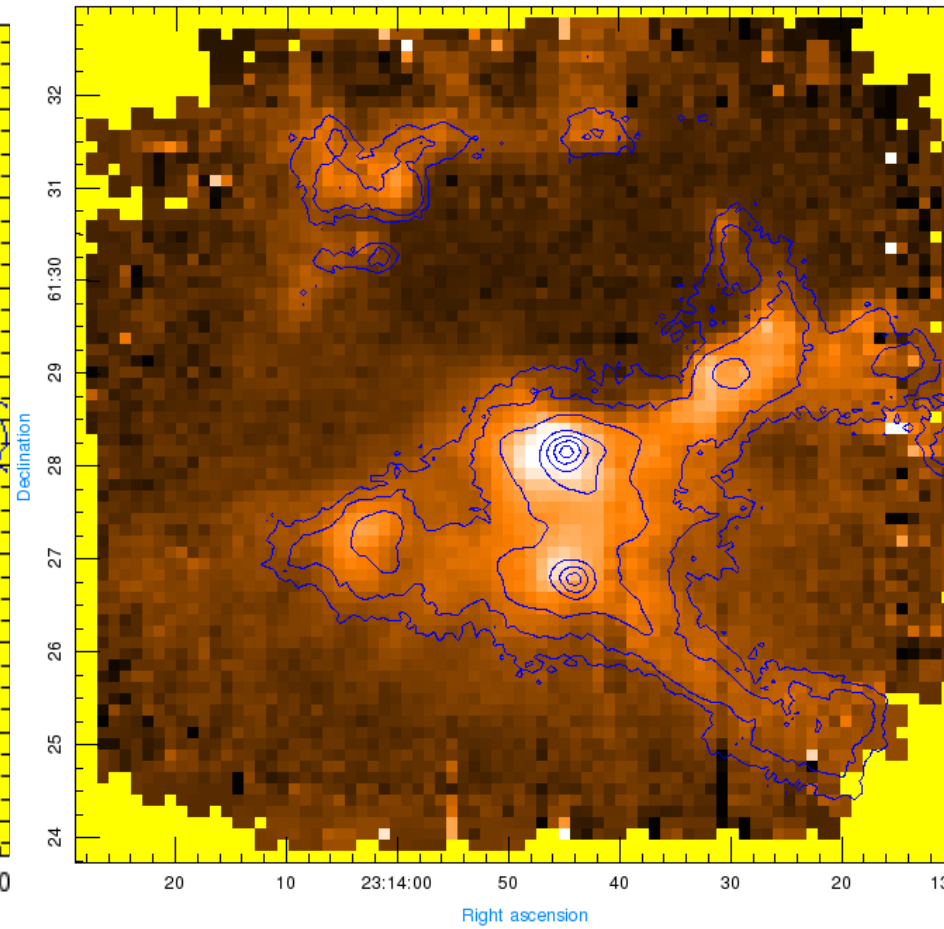
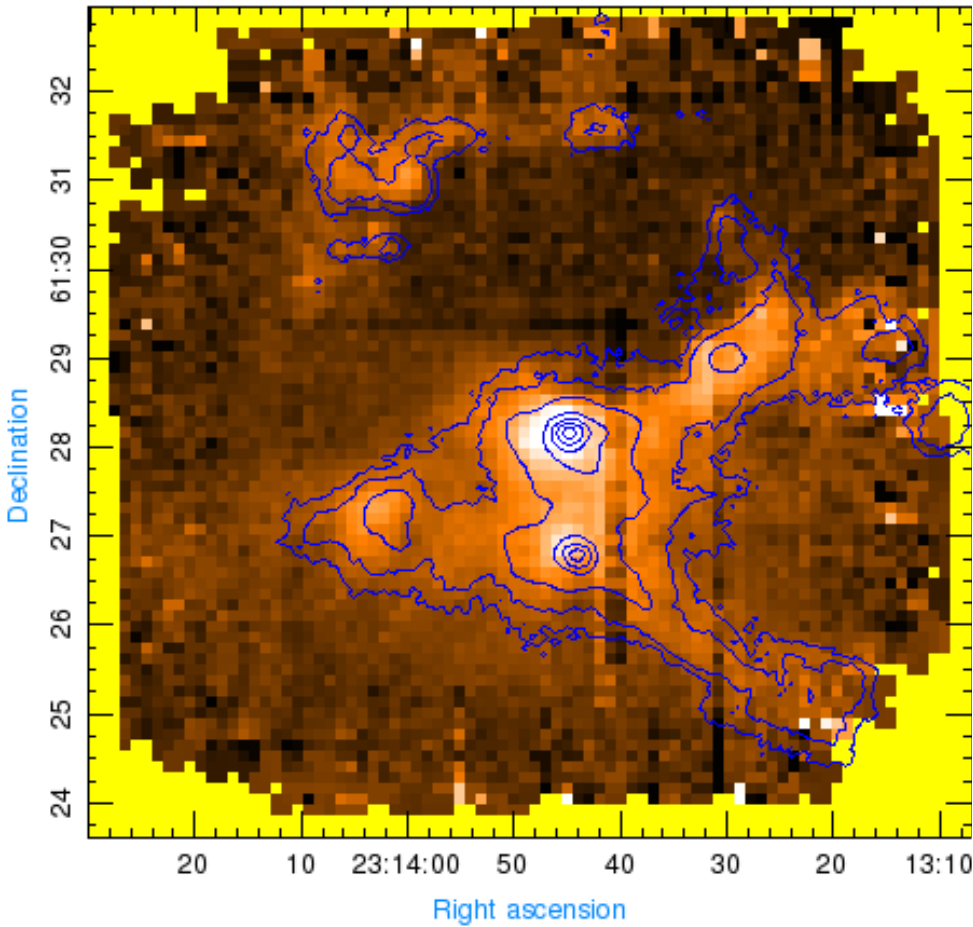
The contour level: 10, 9.61619, 6.15754, 2.69889, 4,1.5

S158A

Range of velocity (-68 _ -40)

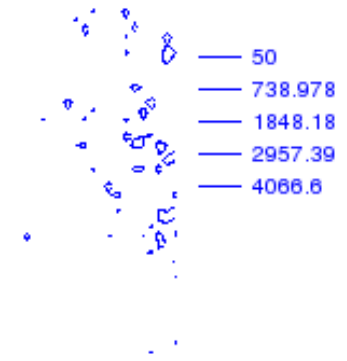
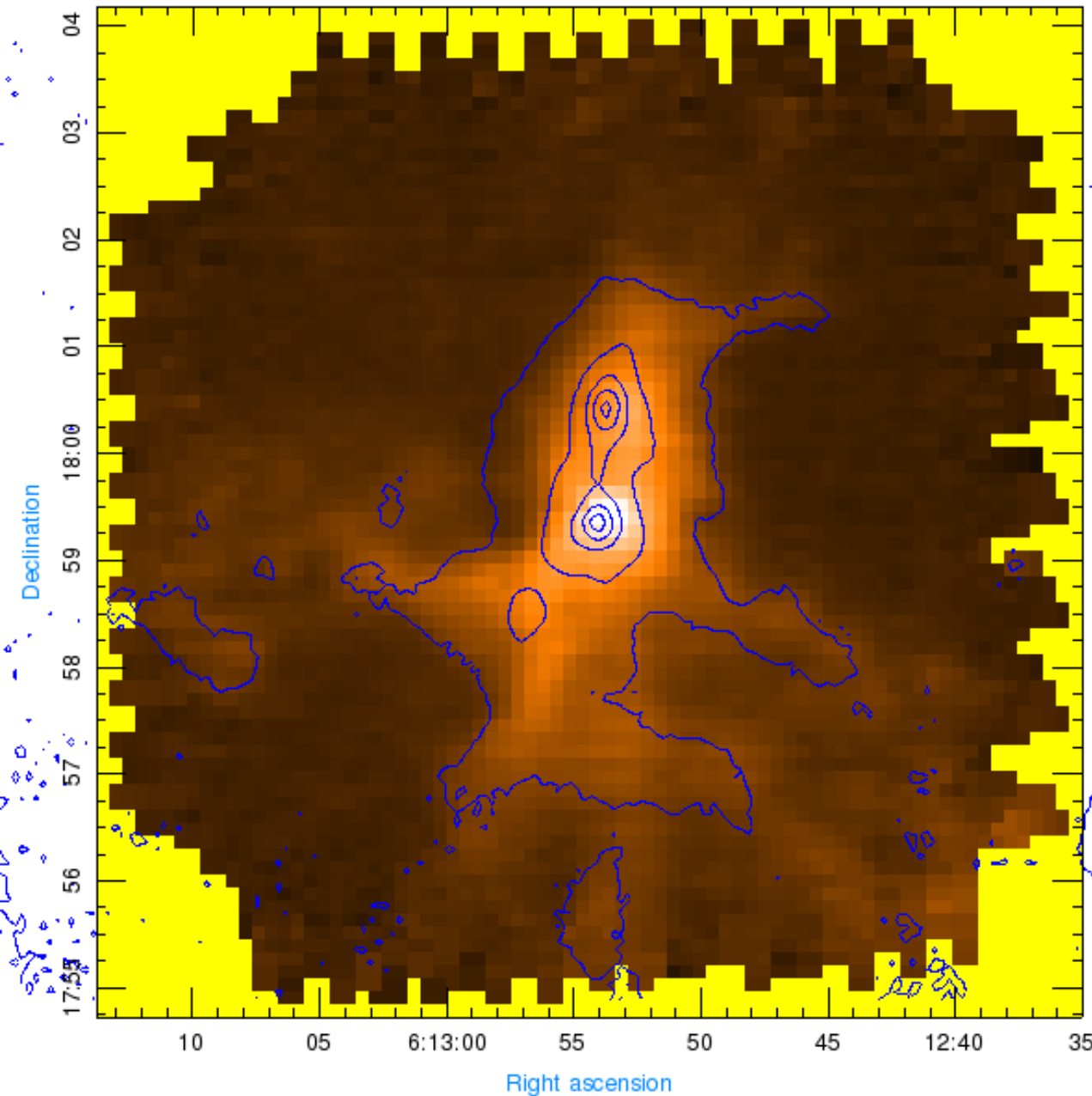
S158 A_13co_850

S158 A_13co(-68_-40)_850



The contour level: 53.5301, 41.4752, 29.4203, 17.3654, 5.31045, 2, 1

S255

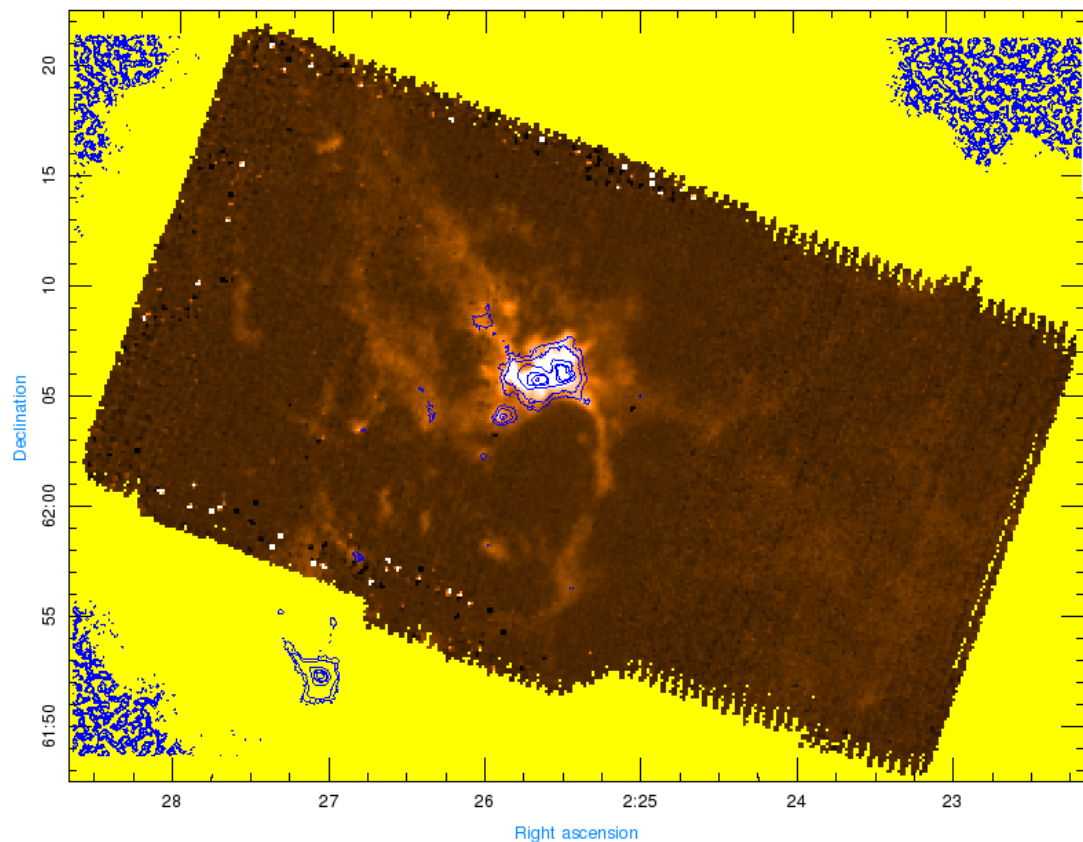
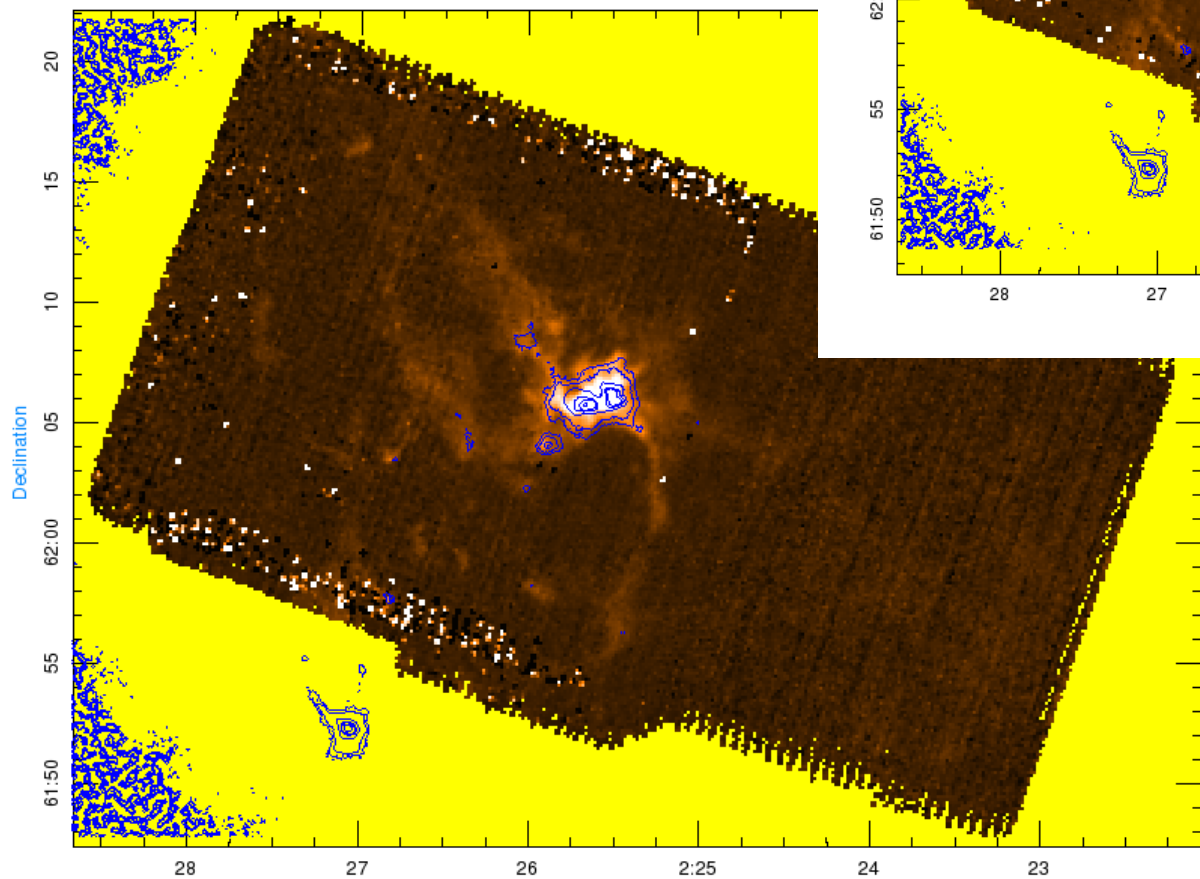


Range of velocity (2_18)

The contour level:
4066.66, 2957.39,
1848.18, 738.978,
50

W3(2)

W3(2)_13co_850

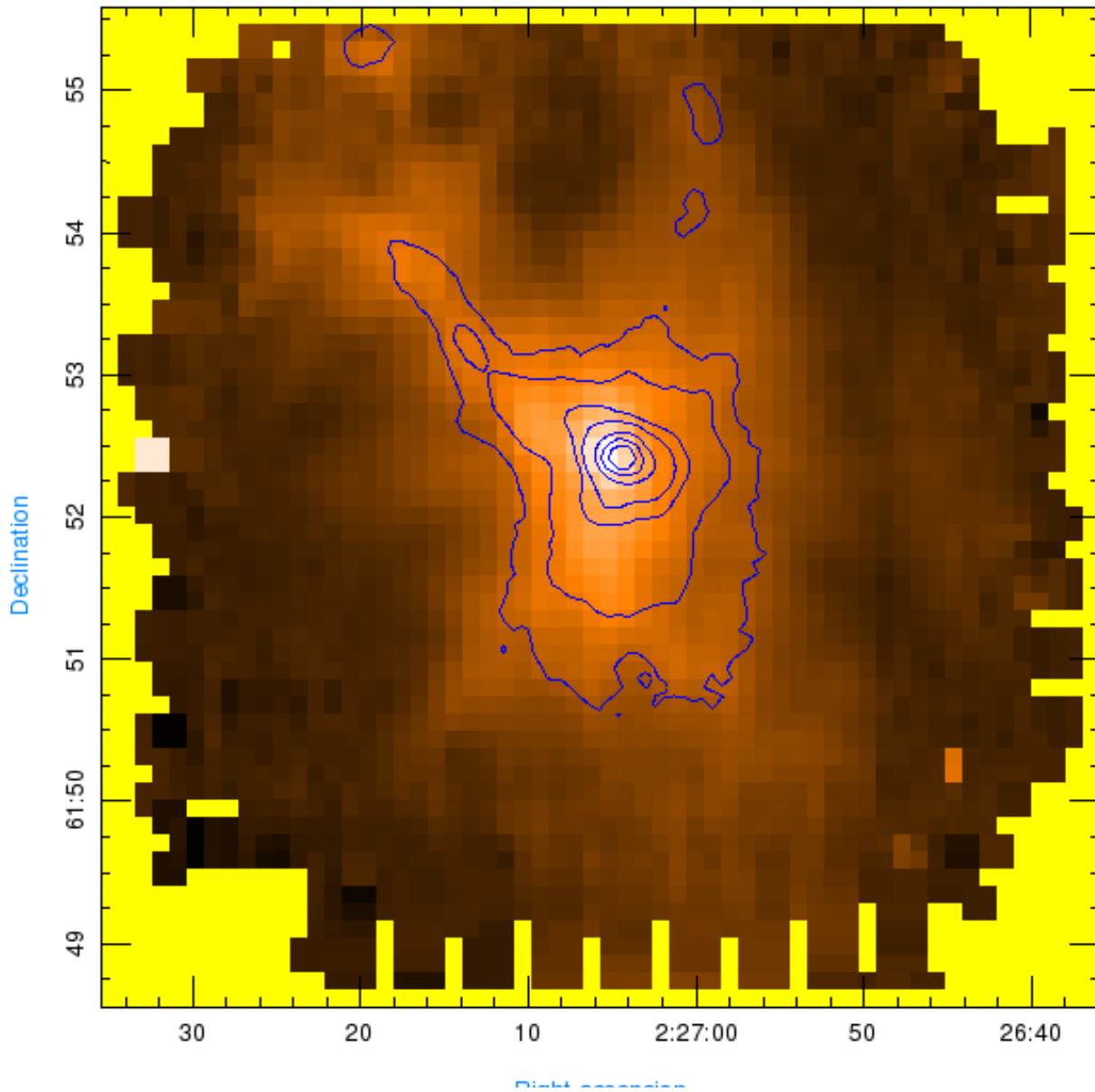


Range of velocity (-48 _ -30)

The contour level: 45, 20, 15,
9, 3, 1.7

W3(OH)_13co(-42_-56)_850

W3OH

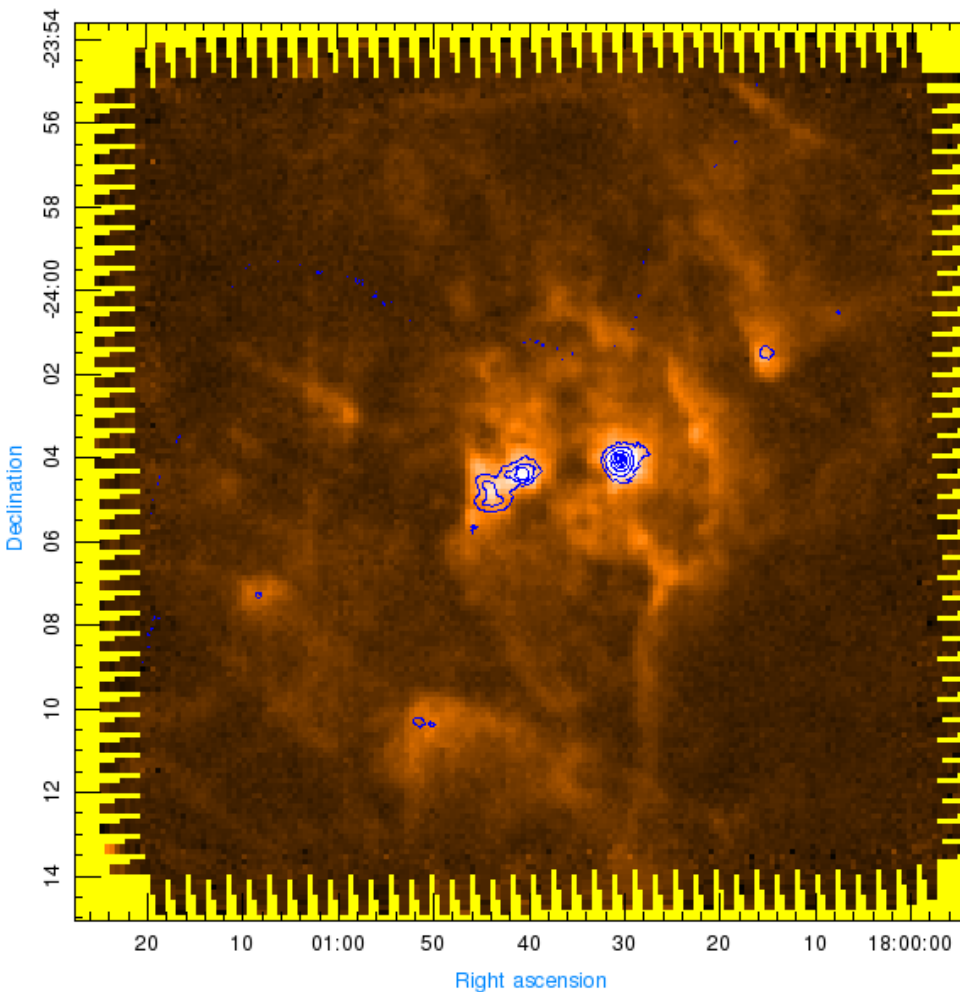


- 10
- 15.0347
- 32.4717
- 49.9087
- 67.3457
- 4
- 1.9

Range of velocity (-42 _ 56)

W28a

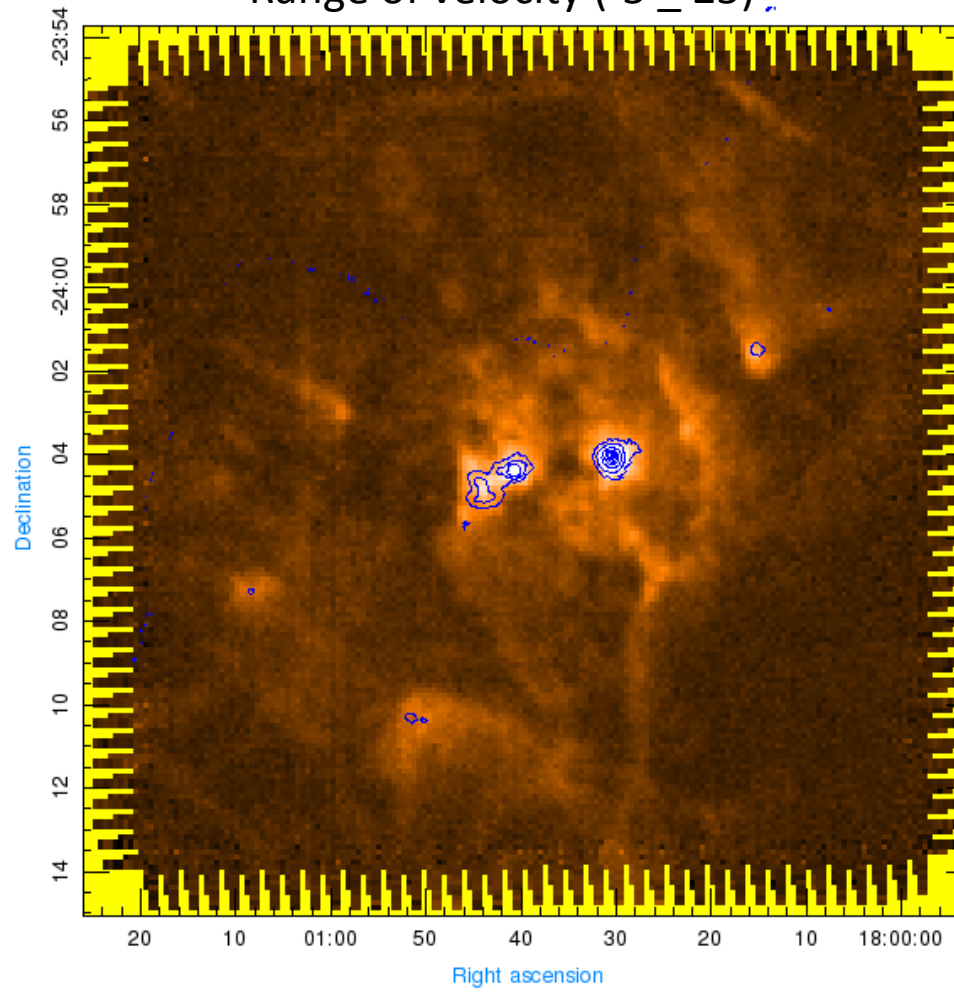
W28A2(1)_13co_850



Right ascension

W28A2(1)_13co(-5_25)_850

Range of velocity (-5 _ 25)

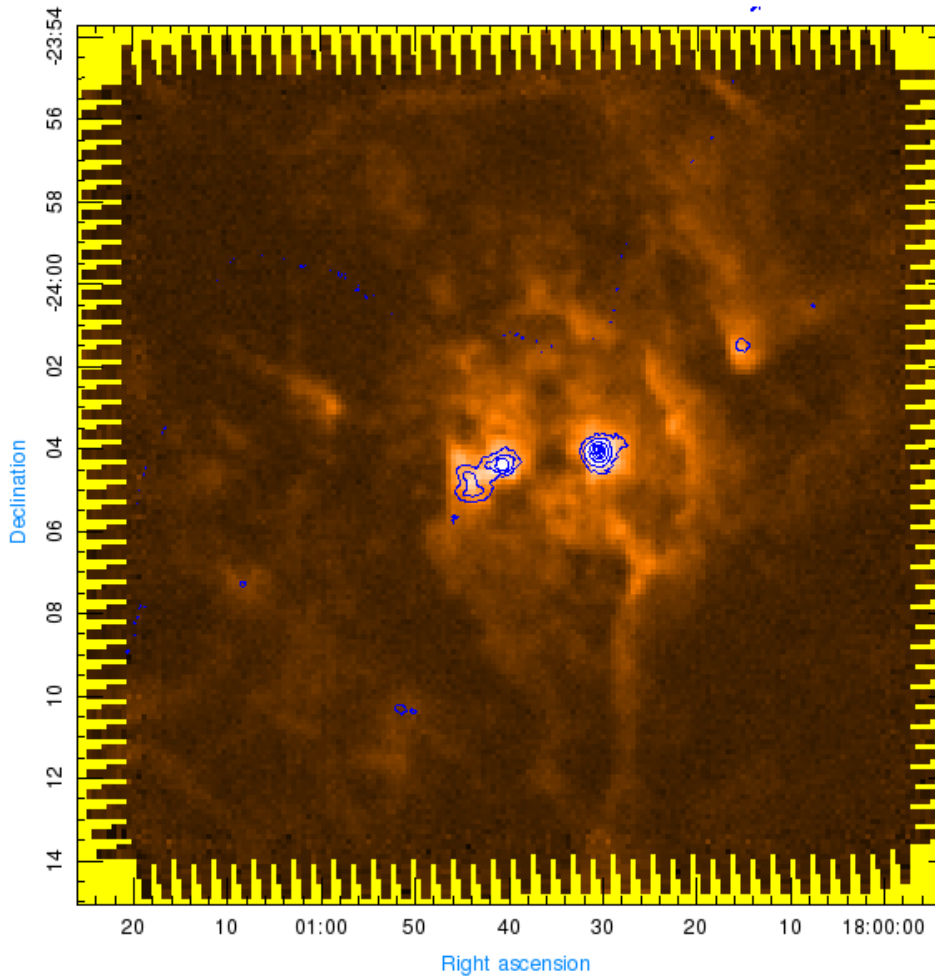


Right ascension

The contour level: 92.5437, 69.025, 45.5062, 21.9875, 10, 5

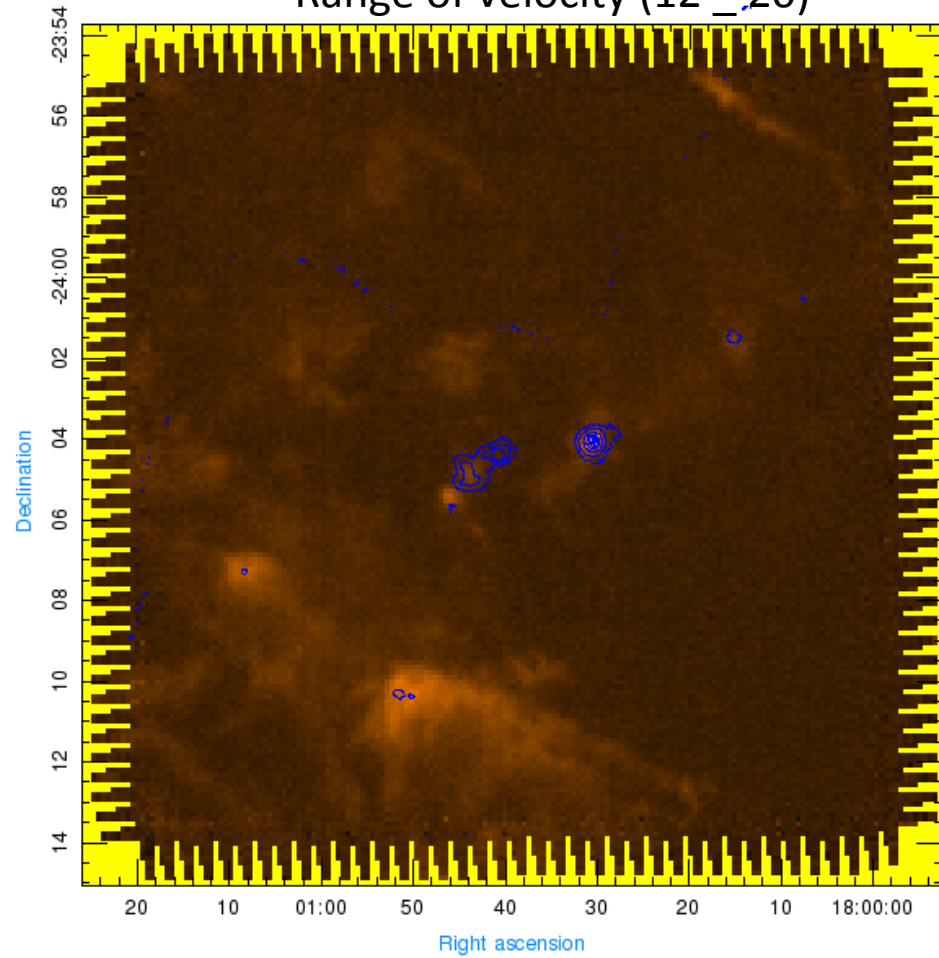
W28a

W28A2(1)_13co(3_15)_850



W28A2(1)_13co(12_20)_850

Range of velocity (12_20)



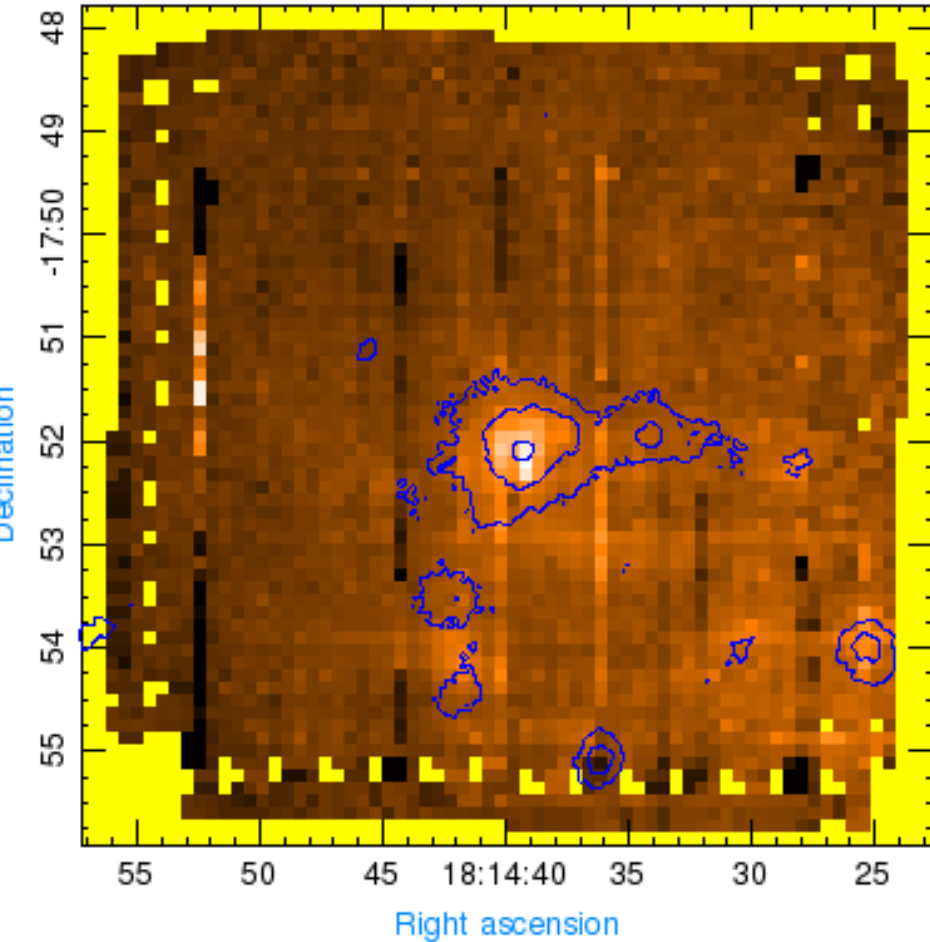
The contour level: 10, 9.61619, 6.15754, 2.69889, 4,1.5

W33A_13co_850

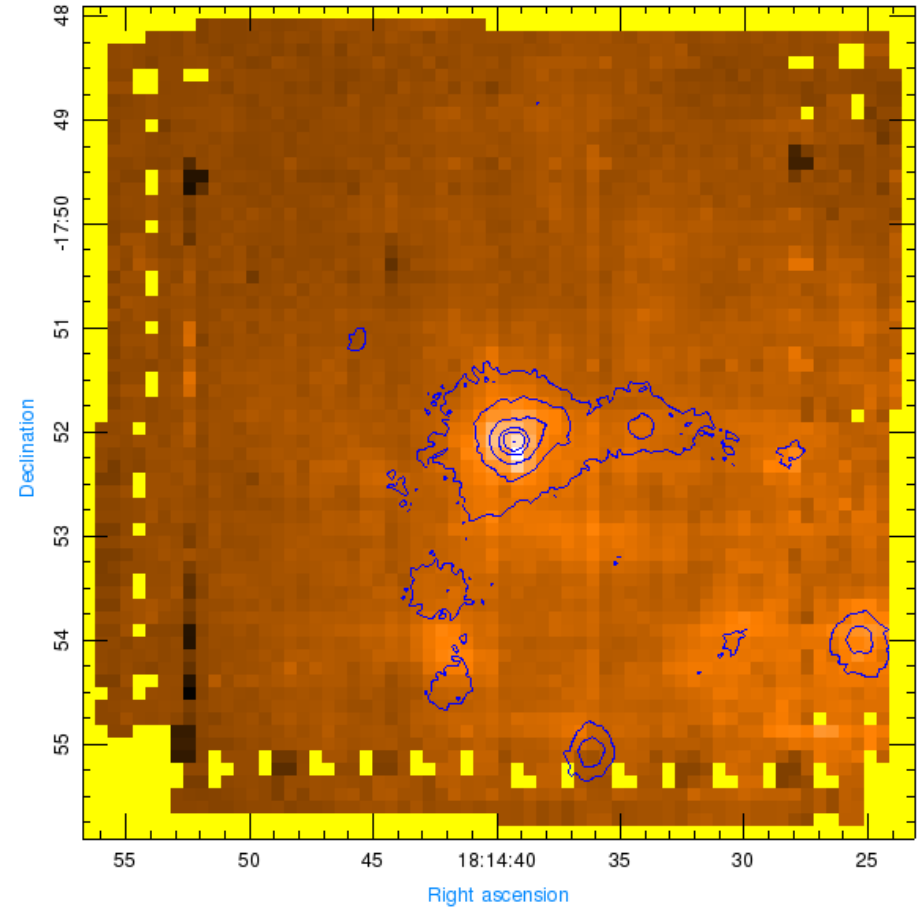
W33A

— 6.96819
24.3255
W33A_13co(25_50)_850

Range of velocity (25 _ 50)



The contour level: 76.3796, 50.0402, 41.6829, 24.3255, 6.96819, 3



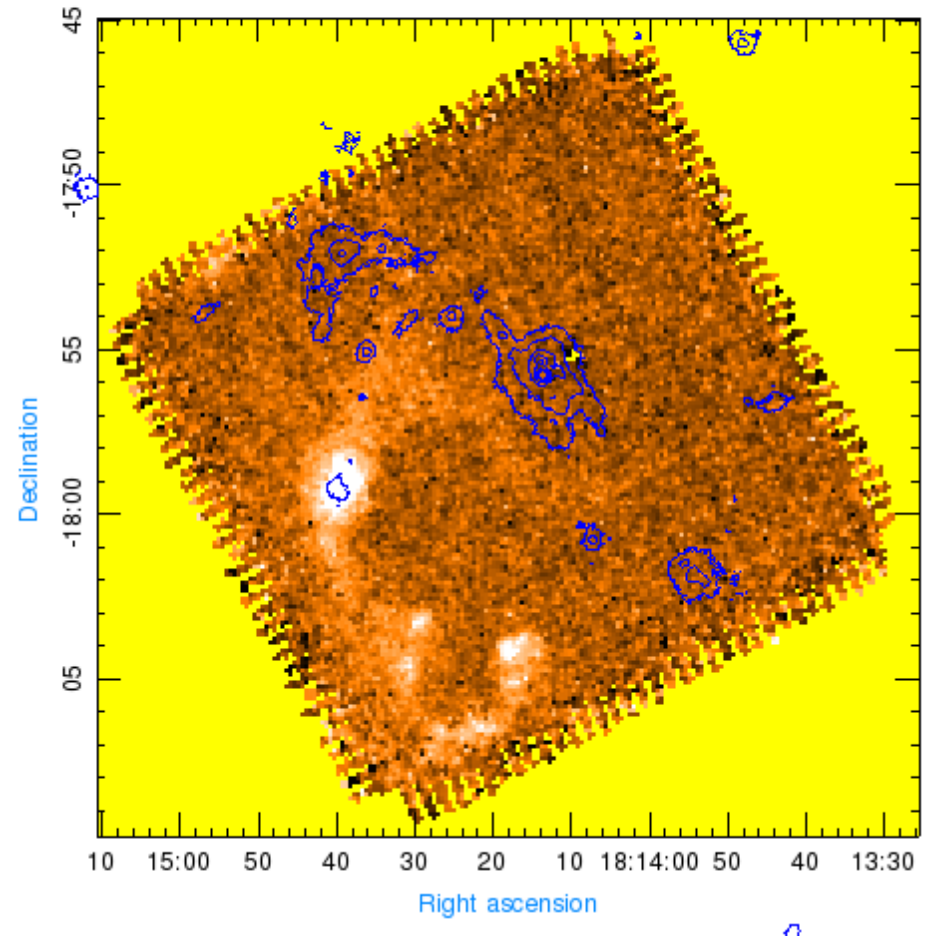
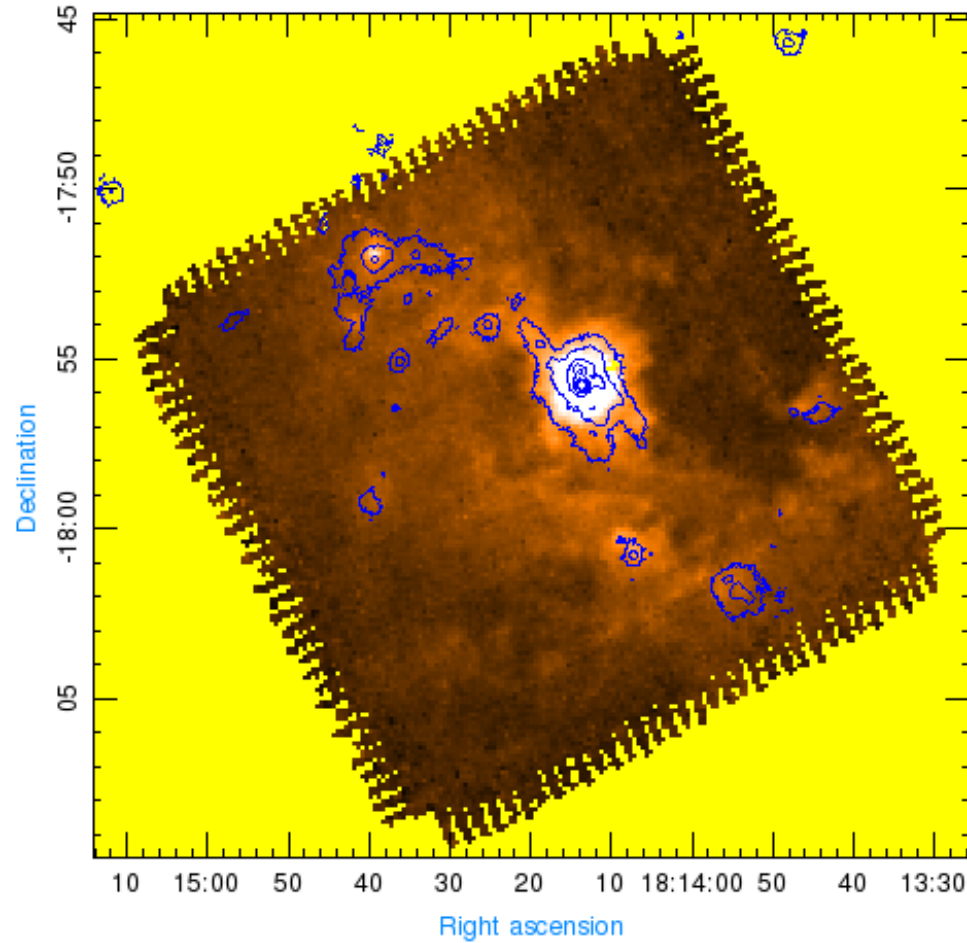
The contour level: 30, 24.3255, 20, 12, 6.96819, 3

W33cont_13co_850

W33cont

W33cont_13co(8_20)_850

Range of velocity (8_20)



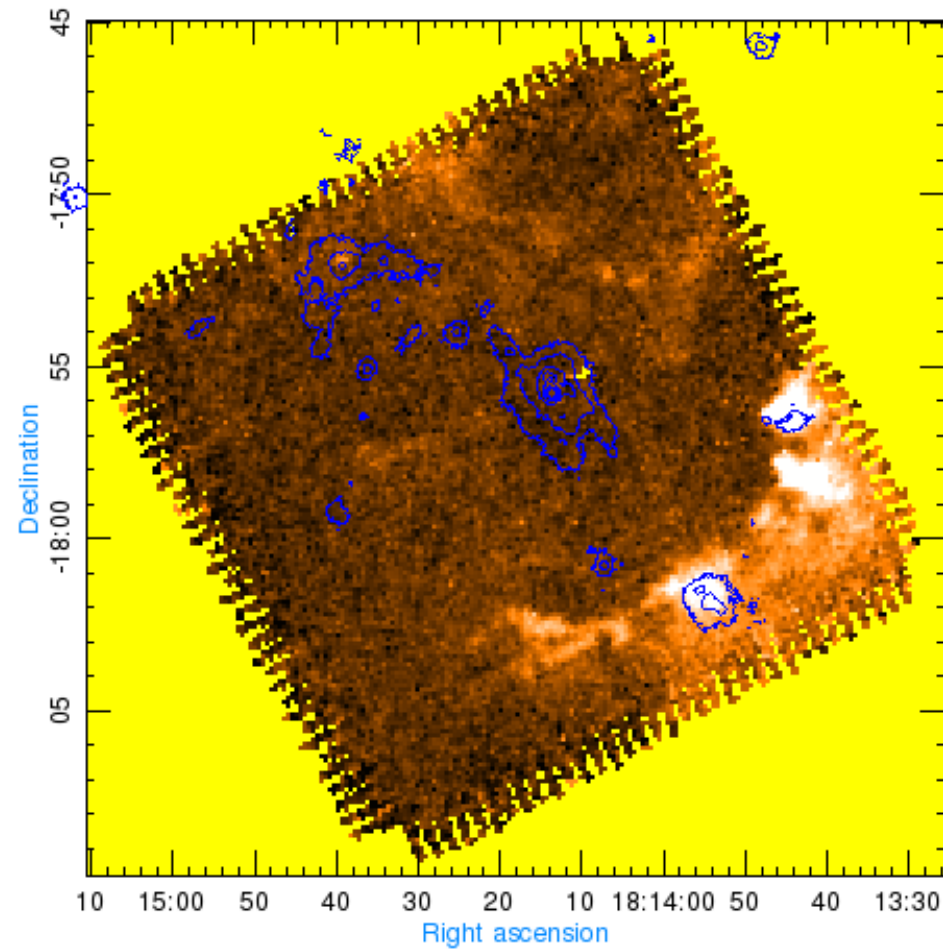
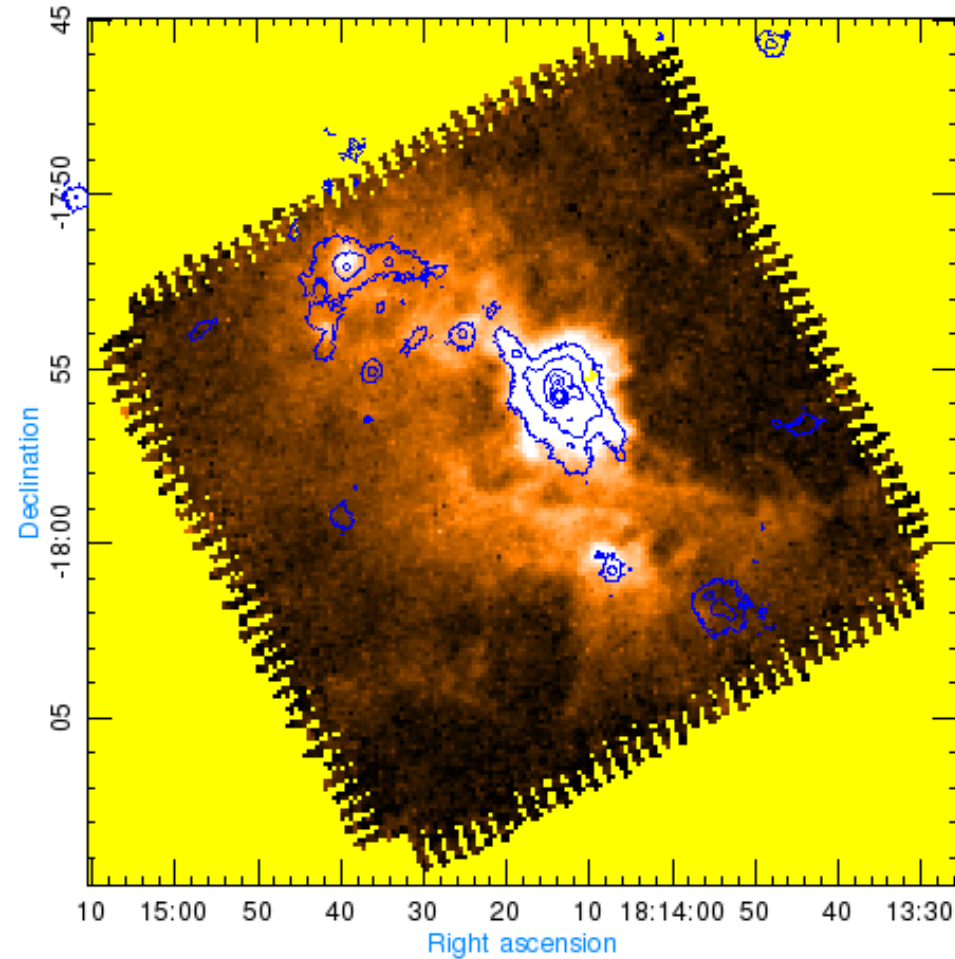
The contour level: 76.3796, 50.0402, 41.6829, 24.3255, 6.96819, 2

W33cont

W33cont_13co(25_48)_850

W33cont_13co(50_60)_850

Range of velocity (50 _ 60)



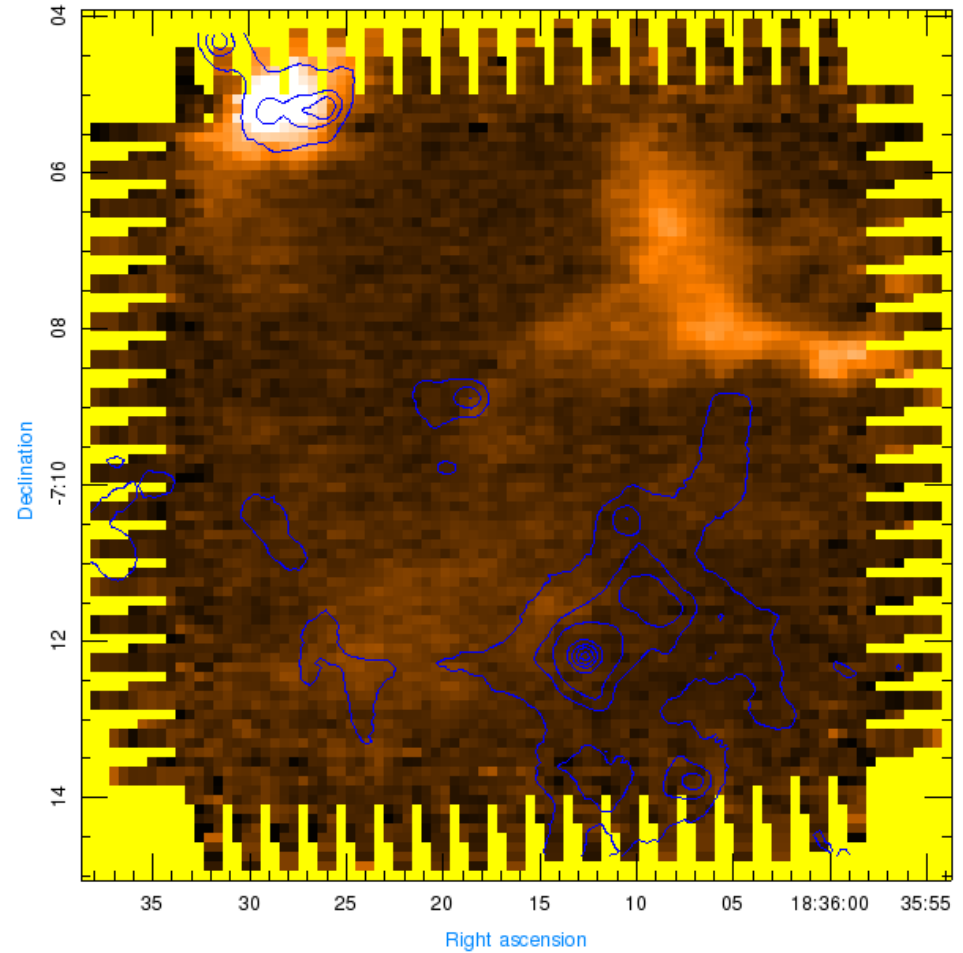
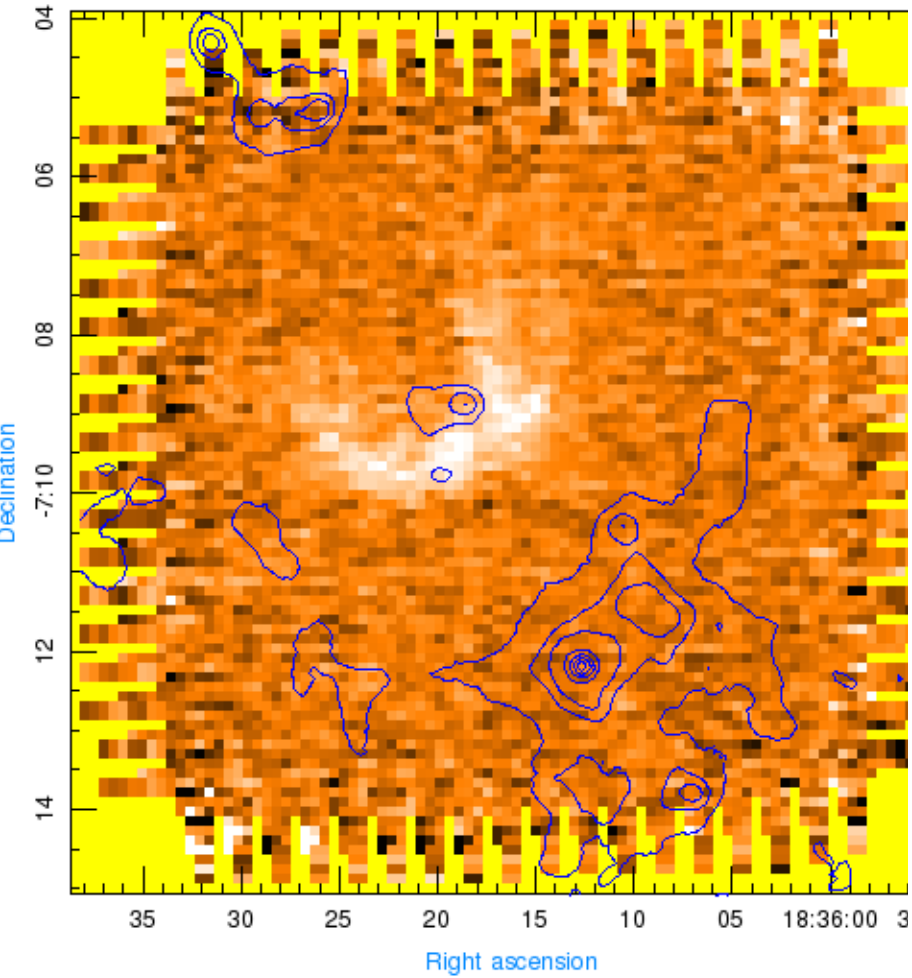
The contour level: 76.3796, 50.0402, 41.6829, 24.3255, 6.96819, 2

W42

W42_13co(74_82)_850

W42_13co(43_48)_850

Range of velocity (43_48)



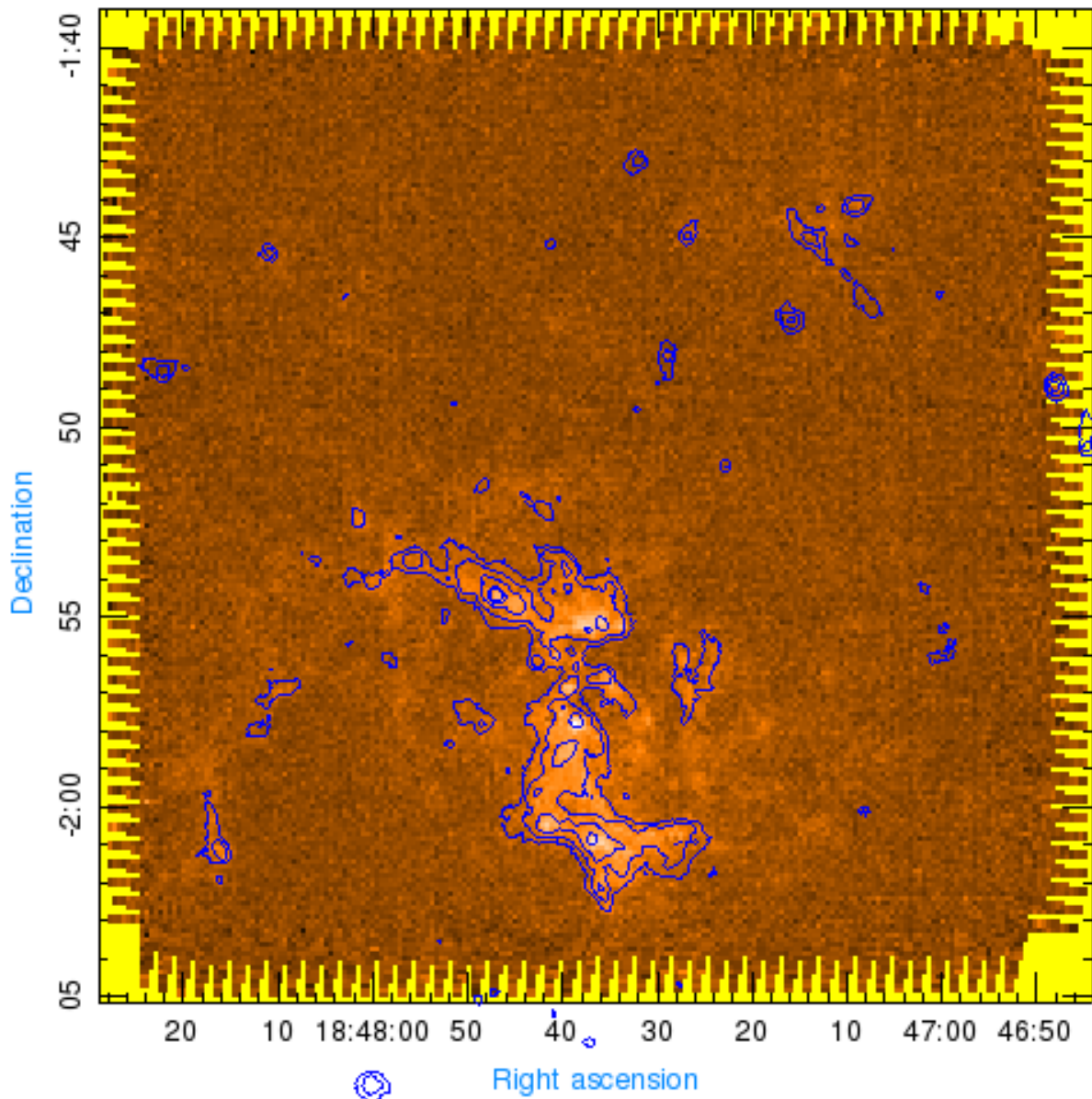
The contour level: 51.3875, 39.9231, 28.4586, 16.9941, 5.52966, 3, 1

W43N_M_13co(82_110)_850

W43N_M

- 9.5763
- 30.5135
- 51.4506
- 4
- 2

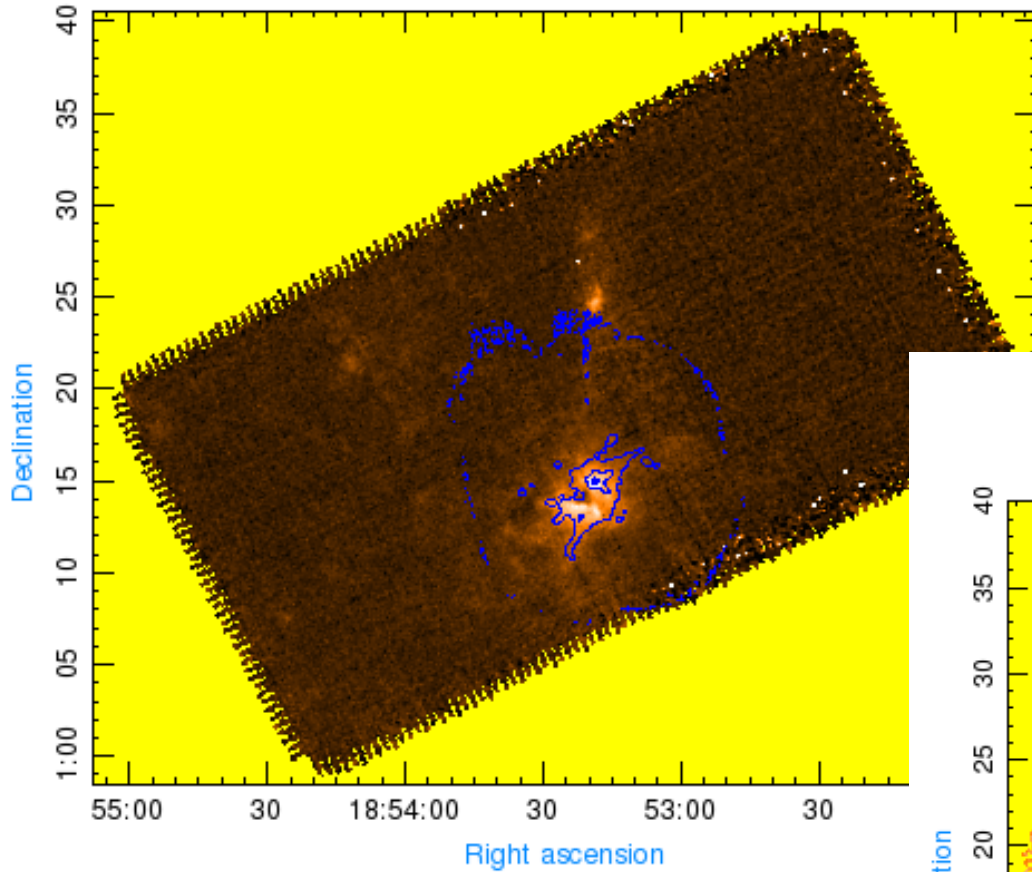
Range of velocity (82 _ 110)



w44_13co_850

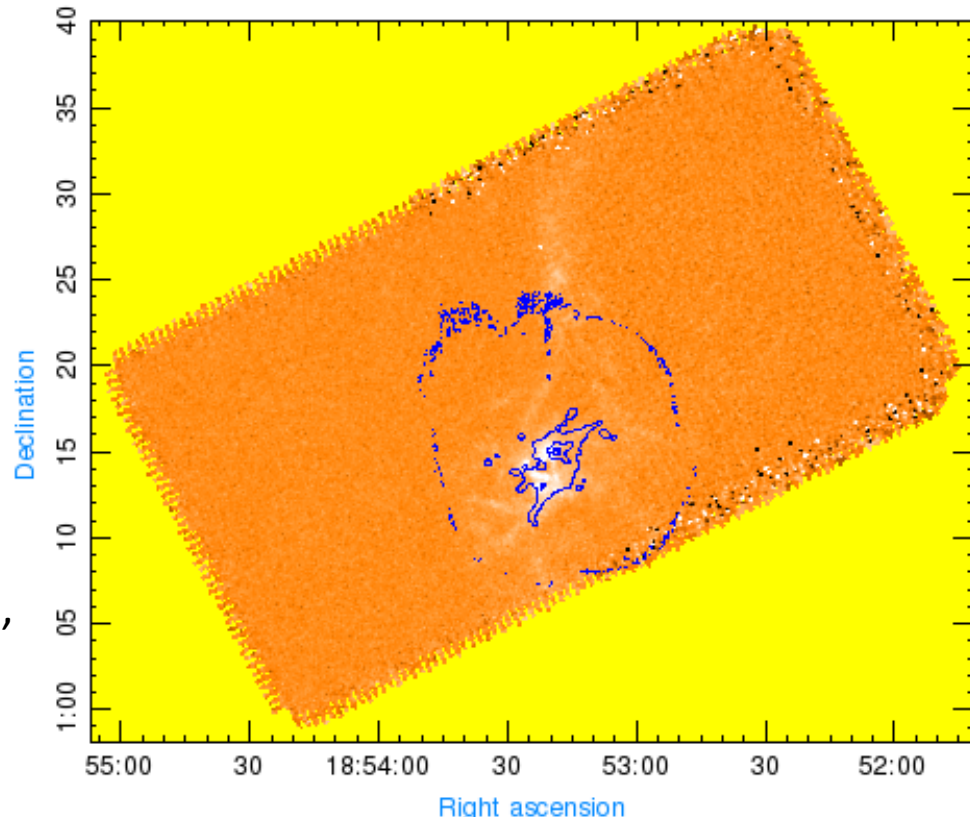
- 2862.42
- 19969.5
- 28523
- 37076.5
- 200

W44



W44_13co(39_48)_850

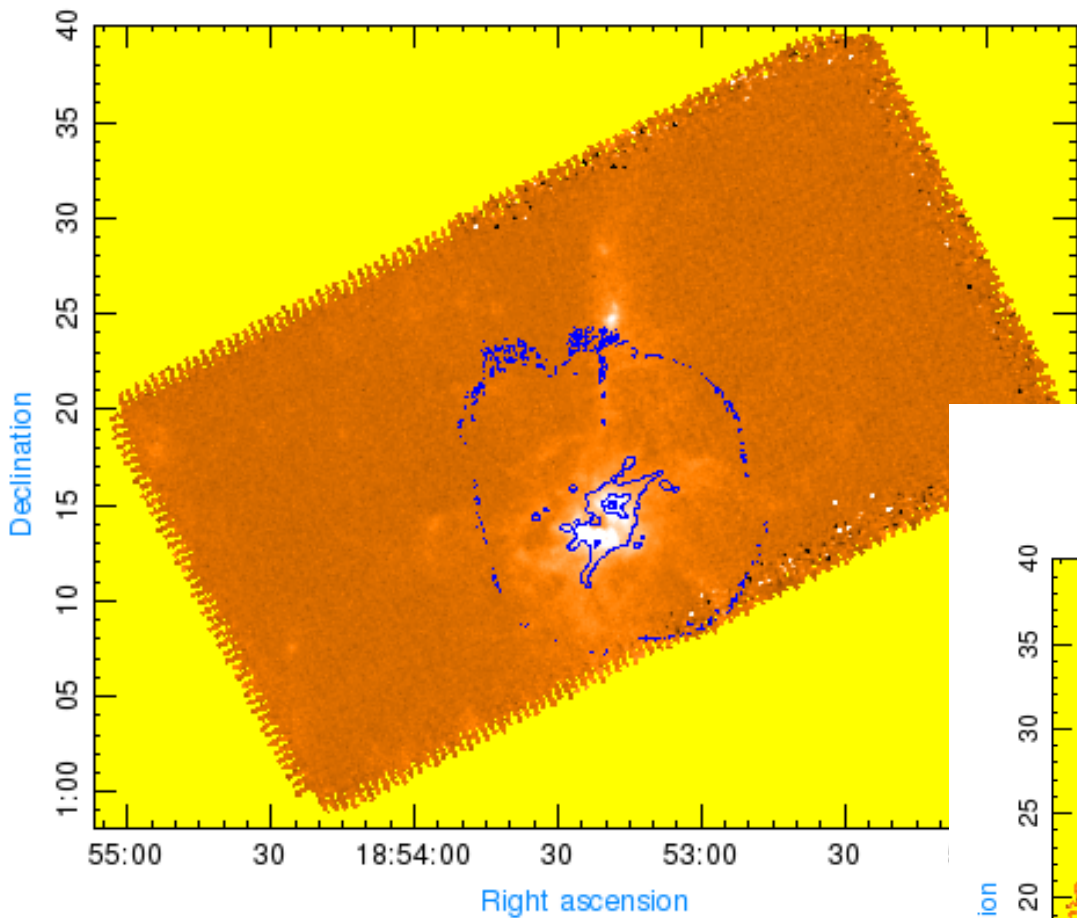
Range of velocity (39 _ 48)



The contour level: 37076.5, 28523, 19969.5, 2862.42, 200

W44_13co(48_65)_850

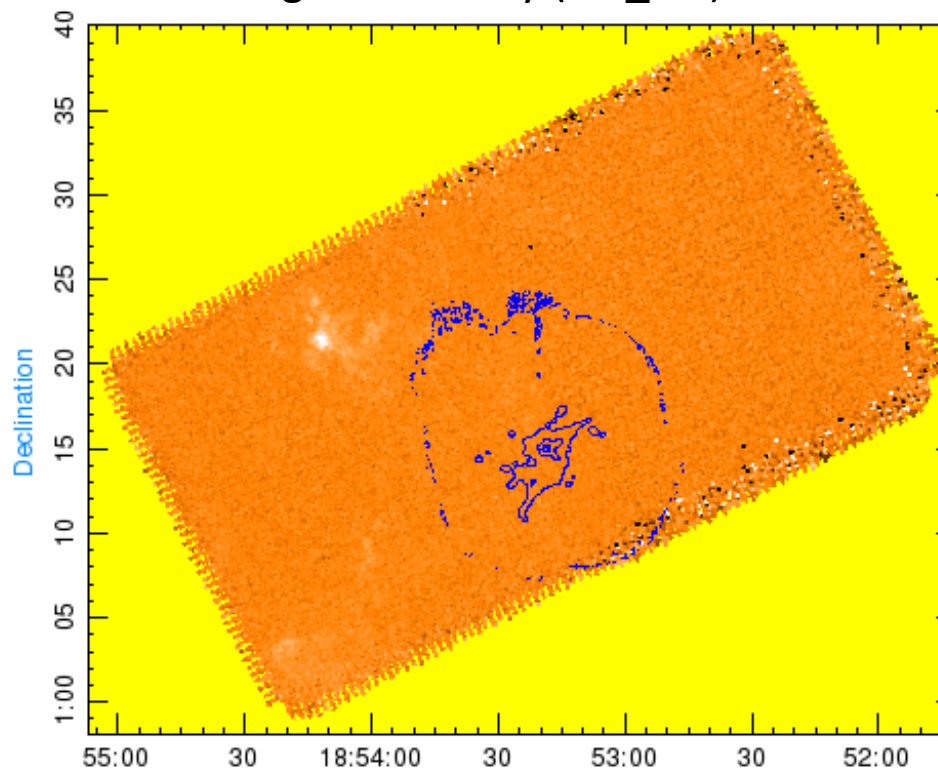
W44



— 2862.42
— 11415.9
— 19969.5
— 28523
— 200

W44_13co(86_95)_850

Range of velocity (86 _ 95)

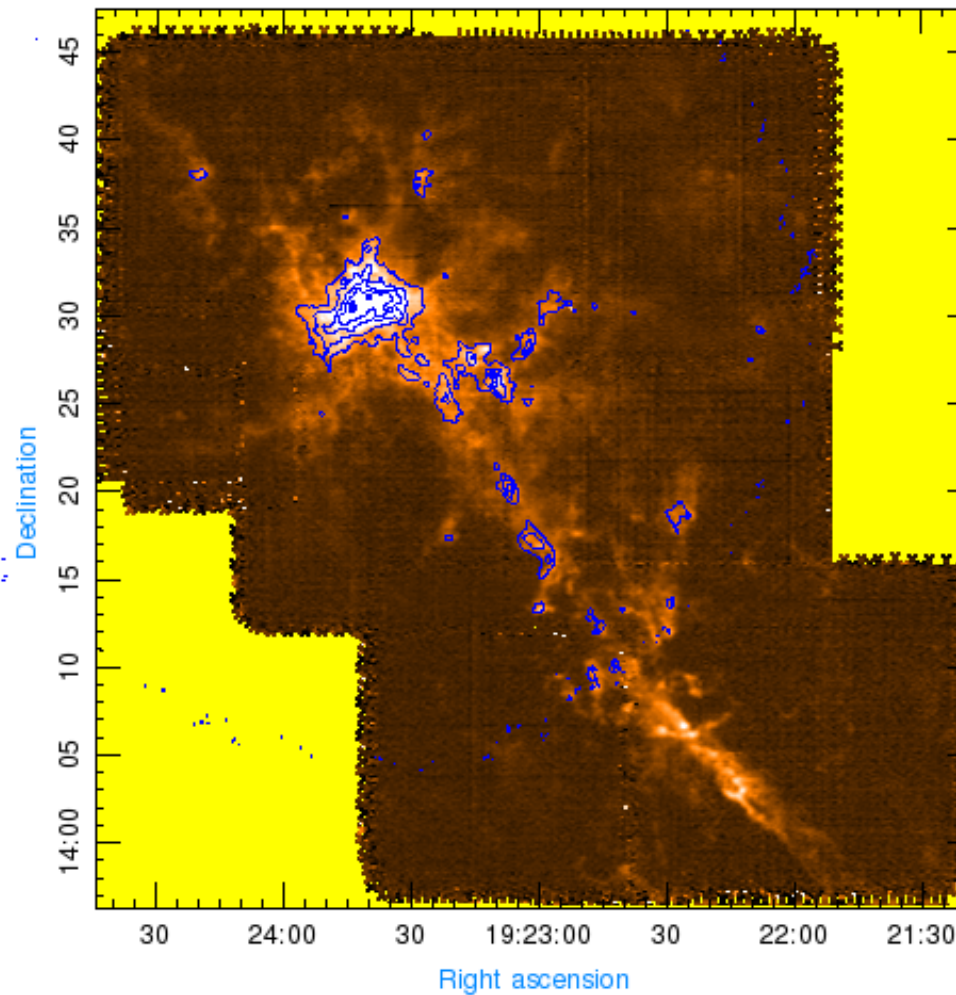
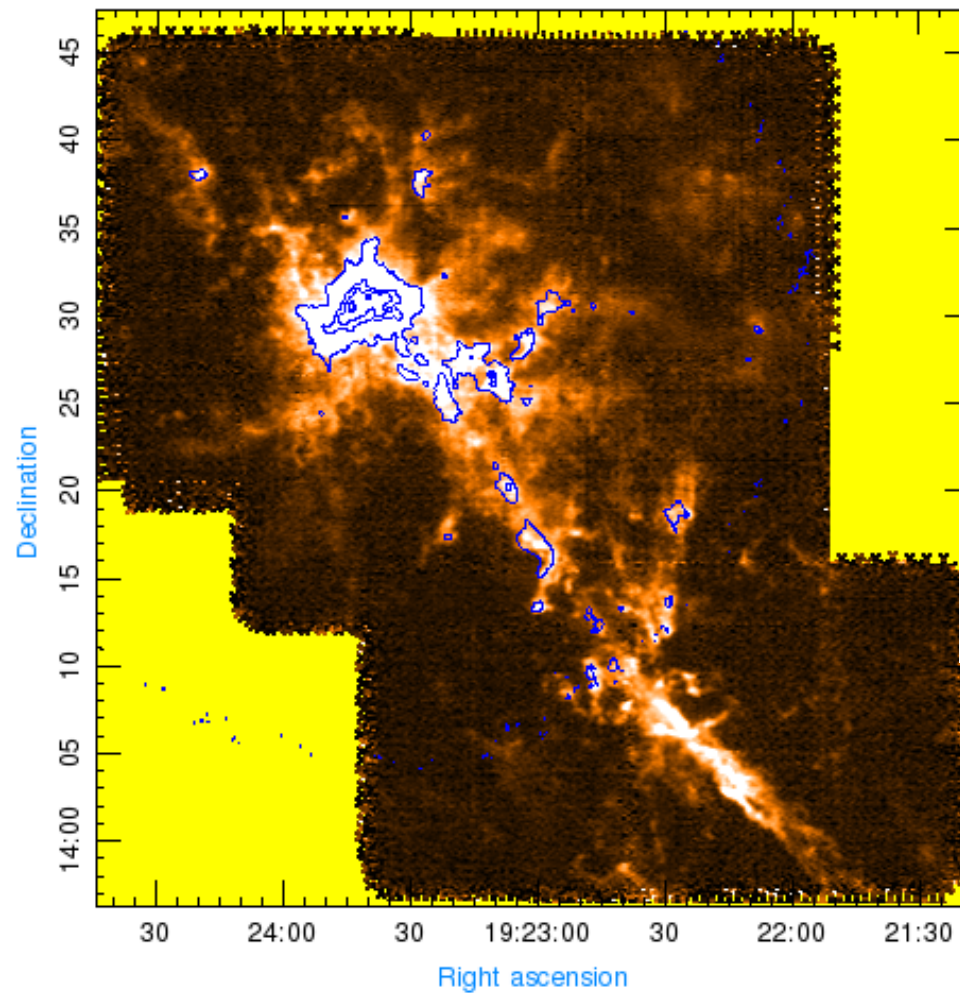


The contour level: 37076.5, 28523, 19969.5, 2862.42, 200

W51

W51_13co(44_76)_850

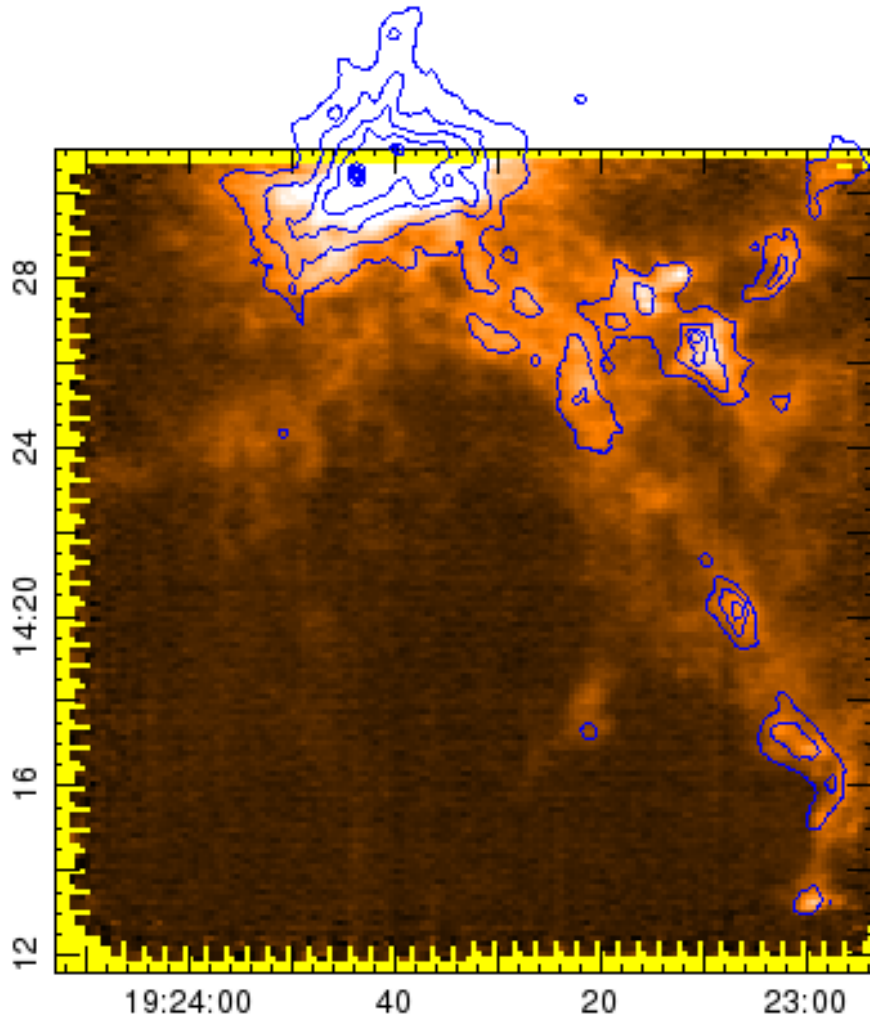
Range of velocity (44 _ 76)



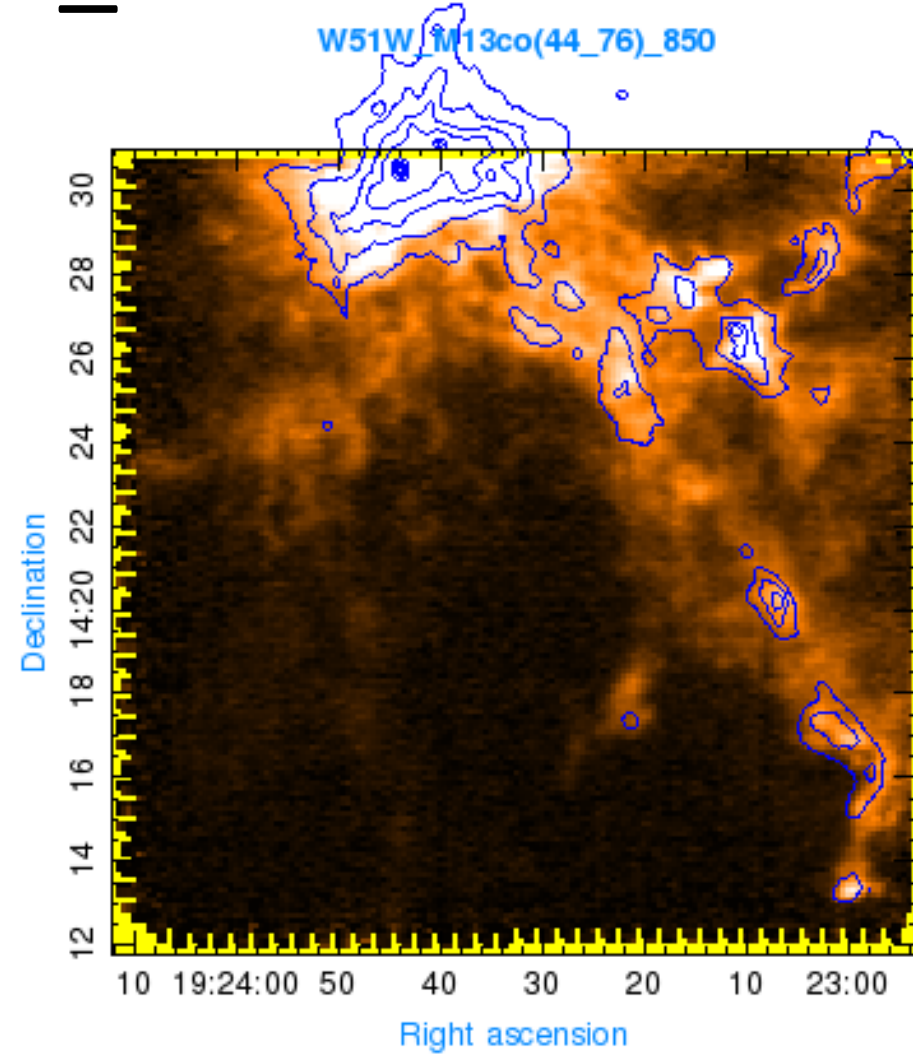
The contour level: 214.07, 165.58, 117.05,
68.5399, 20.0299, 10, 5, 2

W51W_M

W51W_M_13co_850



— 20.8025
- - - -
W51W_M13co(44_76)_850

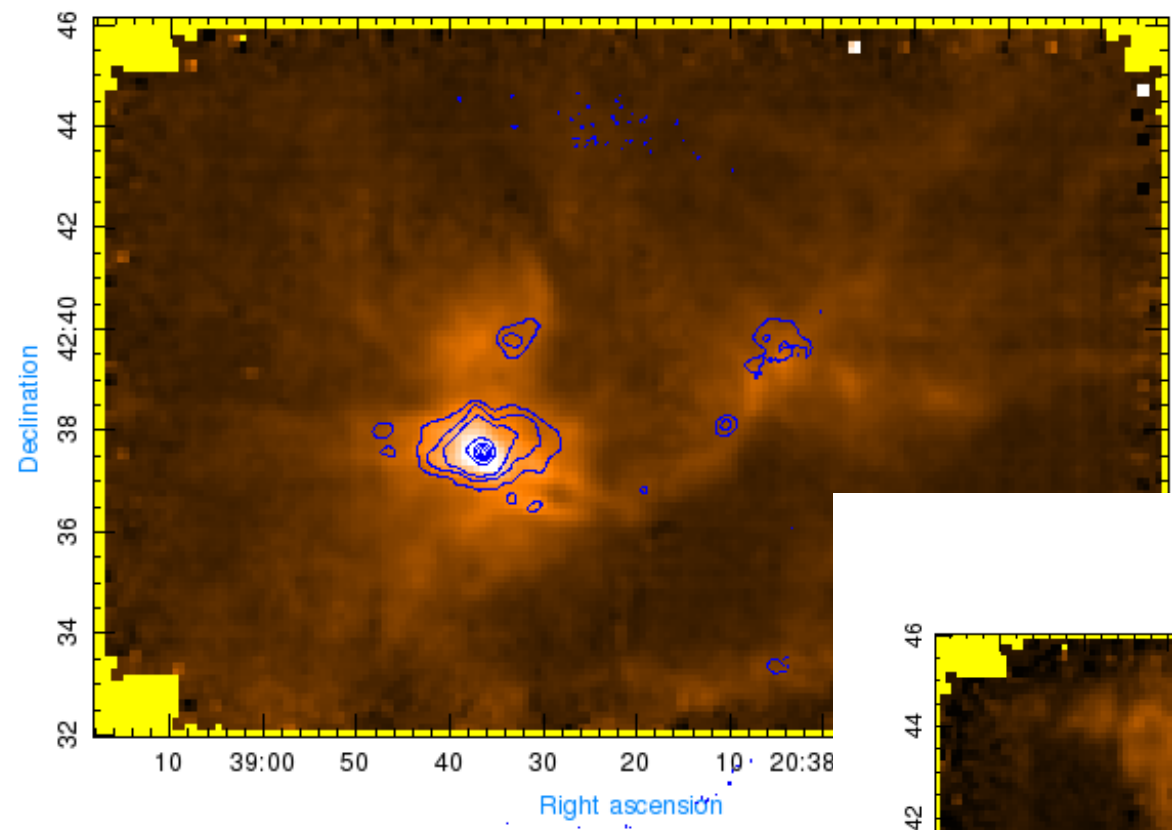


The contour level: 214.07, 165.58, 117.05, 68.5399, 20.0299, 10, 5, 2

W75N_13co_850

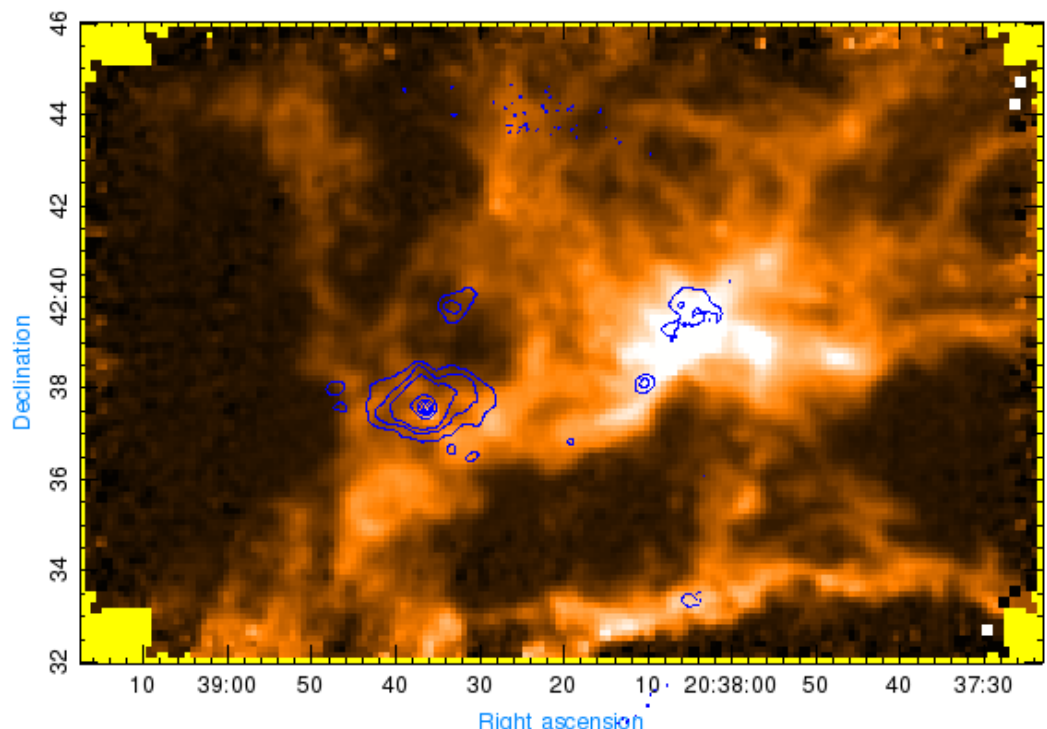
- 4.97042
- 23.2213
- 41.4721
- 59.723
- 77.9738
- 3
- 1.5

W75N



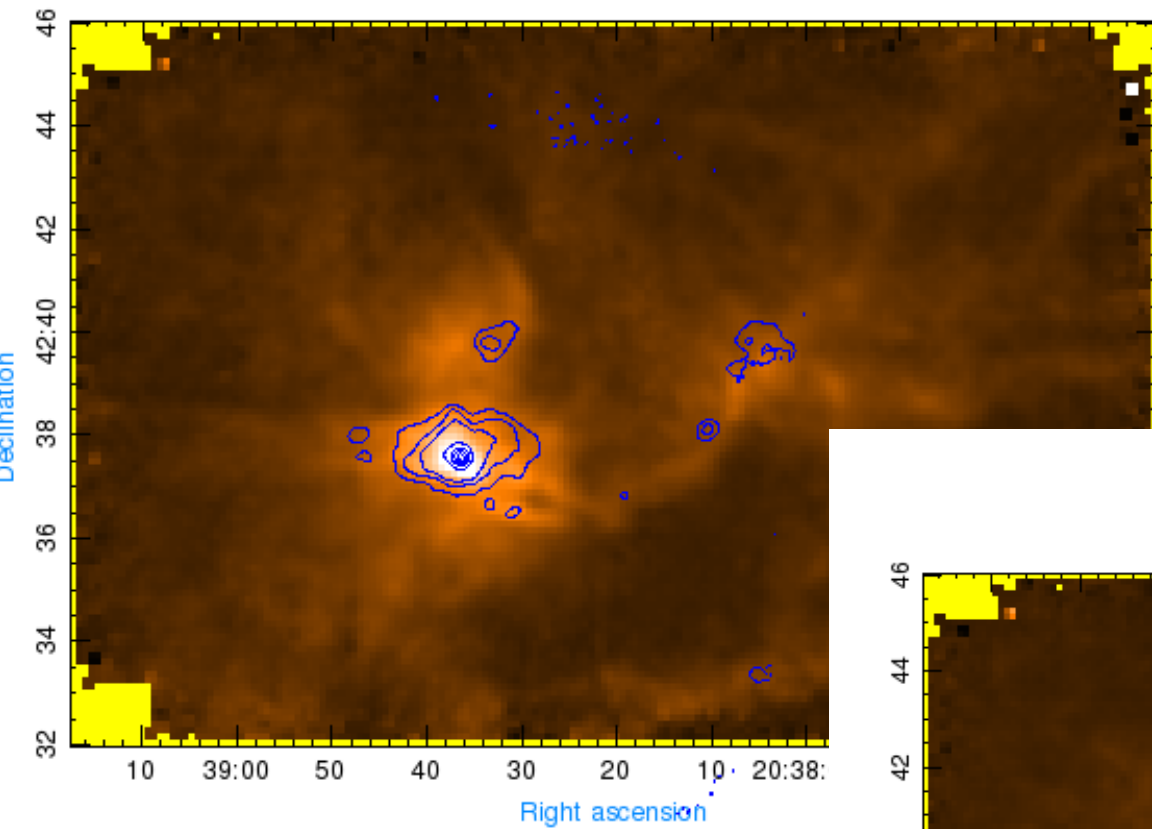
W75N_13co(-5_2)_850

Range of velocity (-5 _ 2)



The contour level: 77.9738, 59.723, 41.4721, 23.2213, 4.97042, 3, 1.5

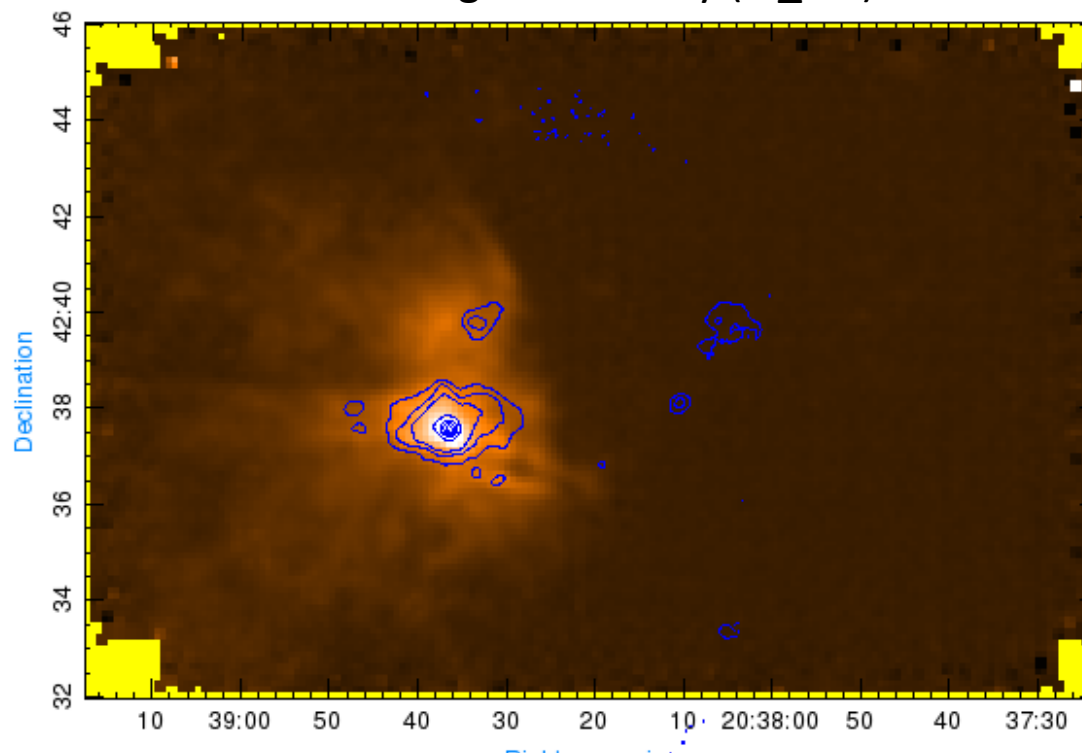
W75N_13co(-8_20)_850



W75N

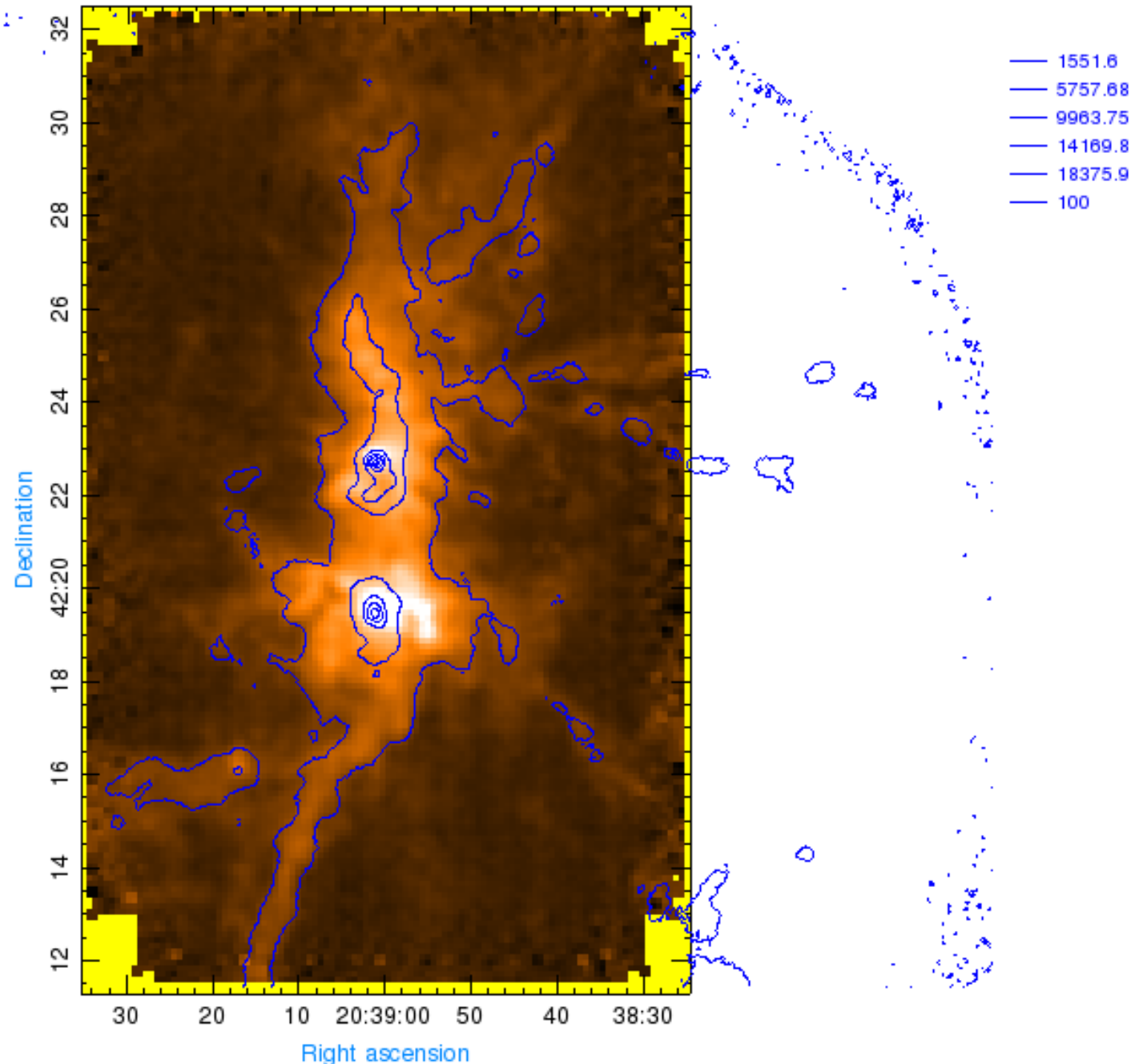
W75N_13co(2_18)_850

Range of velocity (2 _ 18)



The contour level: 77.9738, 59.723, 41.4721, 23.2213, 4.97042, 3, 1.5

W75OH



The contour level:
18375.9, 14169.8,
9963.75, 5757.68,
1551.8, 100

W75(OH)_13co(15_20)_850

Range of velocity (15 _ 20)

W75(OH)_13co(14_22)_850.sdf

W75OH

Range of velocity (14_22)

- 15
- 57
- 14
- 18
- 20

The
contour
level:
18375.9
14169.8
5757.68
1551.8,
100

